EXTRACELLULAR VESICLE SUBPOPULATIONS FROM HTLV-1 INFECTED CELLS INDUCE DIFFERENTIAL EFFECTS IN RECIPIENT CELLS

by

Zachary Cuba

A Thesis
Submitted to the
Graduate Faculty
of
George Mason University
in Partial Fulfillment of
The Requirements for the Degree
of
Master of Science
Biology

Committee:

_____	Dr. Fatah Kashanchi, Thesis Chair
_____	Dr. Lance Liotta, Committee Member
_____	Dr. Ancha Baranova, Committee Member
_____	Dr. Iosif Vaisman, Director, School of Systems Biology
_____	Dr. Donna Fox, Associate Dean, Office of Student Affairs & Special Programs, College of Science
_____	Dr. Fernando R. Miralles-Wilhelm Dean, College of Science
Date: _____	Spring Semester 2022 George Mason University Fairfax, VA

Extracellular Vesicle Subpopulations From HTLV-1 Infected Cells Induce Differential Effects in Recipient Cells

A Thesis submitted in partial fulfillment of the requirements for the degree of Master of Science at George Mason University

by

Zachary Cuba
Bachelor of Science
College of William and Mary, 2020

Director: Fatah Kashanchi, Professor
George Mason University

Spring Semester 2022
George Mason University
Fairfax, VA

DEDICATION

This is dedicated to the mosaic of people throughout my life who have encouraged me and fostered my growth—I am standing here now because of you.
Ad astra per aspera / Concordia res parvae crescunt

ACKNOWLEDGEMENTS

I would like to thank the many friends, relatives, and supporters who have made this happen. Mom and Dad, thank you for always being a stable foundation and a respite for me in this process. My friends, thank you for keeping me sane and in good spirits despite me being holed-up in lab all the time. My undergrad PI, Dr. Williamson, thank you for providing me the hands-on experience of how to perform experiments and inspiring me to pursue microbiology. Thank you to my committee and other professors that I had the honor of learning under for helping me to grow and refine myself as a scientist. Dr Kashanchi, thank you for providing a space and mentorship for me to push myself further than I thought I could go previously. Finally, thank you to the Kashanchi Lab members— especially Heather, James, and Mrs. Gwen—for your scientific, organizational, and emotional support throughout this process. I couldn't have done it without y'all.

TABLE OF CONTENTS

LIST OF FIGURES

LIST OF TABLES

LIST OF ABBREVIATIONS

Adult T-cell Leukemia-Lymphoma ..... ATLL
De-ionized Water……diH_2O
Dulbeco's Modified Essential Medium ..... DMEM
Epidermal Growth Factor Receptor ..... EGFR
Extracellular Vesicle(s)..... EV(s)
Fetal Bovine Serum……FBS
HTLV-1 associated myelopathy/tropical spastic paraparesis ..... HAM/TSP
Human Basic Leucine Zipper Factor……HBZ
Human Telomerase Reverse Transcriptase.....hTERT
Human T-cell Leukemia Virus Type 1 .....HTLV-1
Induced Pluripotent Stem Cells .....iPSCs
Long Terminal Repeat……LTR
Messenger RNA……..…mRNA
Mammalian target of Rapacysin…….mTOR
Mesenchymal stem cells……..MSCs
Multi-Vesicular Bodies…….……..MVBs
Phosphate Buffered Saline……..PBS
Primary Blood Mononuclear Cells…….……..…….PBMCs
Relative Light Units.....RLU
Reverse Transcriptase-Quantitative Polymerase Chain Reaction.....RT-qPCR
Vascular Endothelial Growth Factor……...……VEGF

ABSTRACT

EXTRACELLULAR VESICLE SUBPOPULATIONS FROM HTLV-1 INFECTED CELLS INDUCE DIFFERENTIAL EFFECTS IN RECIPIENT CELLS

Zachary Cuba, M.S.

George Mason University, 2022

Thesis Director: Dr. Fatah Kashanchi

Human T-cell Leukemia Virus Type 1 (HTLV-1) is the causative agent of Adult T-Cell Leukemia/Lymphoma (ATLL) and HTLV-1 associated myelopathy/tropical spastic paraparesis (HAM/TSP). Extracellular vesicles (EVs)—membrane-bound vesicles excreted by cells into the microenvironment which play an extensive role in cell-to-cell communication—have been implicated in contributing to these two conditions by carrying cellular materials from donor cells to recipient cells. Our lab has previously shown that EVs from ATLL cells contain viral protein and mRNA and promote cell-to-cell contact when placed on uninfected recipient CD4+ T-cells, enhancing HTLV-1 infectivity. Another recent paper involving ATLL EVs resulted in mesenchymal stem cell proliferation and was attributed to helping aid in leukemic progression. Because ATLL is a leukocytic cancer, ATLL EVs have the potential to interact with any cells that blood or biofluids

interact with. However, a gap in knowledge exists relating to how ATLL EVs interact with differentiated non-leukocytes. In addition, many of the conclusions made about the effects of cancer "extracellular vesicles" look at a small subpopulation within the total EV population, and have not been generalized. Therefore, in this study, we sought to better understand the different impacts of individual ATLL EV subpopulations upon non-leukocytes. We found that differential ultracentrifugation subpopulations (2K, 10K, 100K, 167K (4hr) and 167K (16hr)) of HuT102 EVs contained different distributions of viral proteins, viral mRNA, and vesicle-associated proteins. We saw that HeLa cells treated with EV subpopulations had no change in cell viability but had preservation of normal cell morphology post-confluency and had different patterns of anchorage-dependent proliferation. Furthermore, we found that less-dense EV subpopulations 100K and 167K (16hr) helped promote anchorage-independent proliferation. Collectively, our data suggests that there may be a correlation between subpopulations with high amounts of vesicle markers and anchorage-dependent proliferation, while subpopulations with low amounts of viral markers may promote anchorage-independent proliferation. These findings prompt further research into how the contents of each ATLL subpopulation affect recipient cell proliferation and whether these recipient cells are pushed towards cancer development.

INTRODUCTION

Human T-cell Leukemia Virus Type 1 (HTLV-1) was the first oncogenic retrovirus to be discovered in humans, and was discovered three years prior to fellow retrovirus Human Immunodeficiency Virus 1 (HIV-1) [1,2]. HTLV-1 is typically transmitted from one person to another through sharing infected biofluids, including breastmilk, sexual fluids, and blood [3]. In most cases, effective transmission requires cell-to-infected cell contact, as the number of free HTLV-1 virions is low, especially compared to HIV-1[4,5]. Based on available data, the infected population is estimated to be 5-10 million, largely endemic to Japan, Sub-Saharan Africa, South America, and the Caribbean. However, it has been noted that many high population areas, remote areas, and minority-majority areas have been understudied [6].

HTLV-1 causes the onset of several diseases, including Adult T-Cell Leukemia/Lymphoma (ATLL) and the neurodegenerative inflammatory condition "HTLV-1 associated myelopathy/tropical spastic paraparesis", also known as HAM/TSP [3,7,8]. Infection contributes to an estimated overall mortality rate of 5-10%; individuals with HAM/TSP have more than double the mortality rate as compared to the entire population of infected individuals [9,10]. However, considering the global lack of local diagnostic medical care and that 95% of infected individuals are seemingly asymptomatic for ATLL and HAM/TSP but may suffer from other conditions, the overall mortality rate

that can be tied to HTLV-1 may be severely undercounted [11–13]. Indeed, HTLV-1 infection is also a predictor of several rheumatic and eye conditions, autoimmune disorders, and opportunistic infections [3,12].

HTLV-1 Oncoproteins

Amongst the suite of HTLV-1 accessory proteins, two are most closely connected with the induction of ATLL: Tax and HBZ. Tax's chief role is acting as a transcriptional activator, as it interacts with multiple transcription factors and increases NF-κB activation[14,15]. This leads to cell cycle progression, ignorance of DNA damage, chromatin remodeling, and IL-13 mediated inhibition of CTL tumor surveillance, allowing for neoplastic transformation of T-cells [15–20]. Tax's transformative properties have even been shown to transform rat fibroblasts by itself when cloned into plasmids [21,22]. More recently, Tax's NF-κB activation has been shown to deregulate/increase autophagy while at the same time preventing autophagosome-lysosome fusion; this accumulation of autophagosomes within the cell has been shown to increase HTLV-1 virion production [23].

Although Tax had been thought to be the major T-cell transforming factor due to its pleiotropic nature, since 2006, HBZ's shared role in leukemogenesis has become more apparent. HBZ, or Human Basic Leucine Zipper Factor, is translated from an antisense transcript in the pX region. Interestingly, while the HBZ protein has been found to work contrary to Tax and slow down T-cell proliferation, the *hbz* mRNA has been shown to have a proliferative effect upon cells [24]. HBZ protein has been shown to act as an antagonist to the formation of Tax-mediated 5' LTR transcription complexes, preventing HTLV-1

transcription [25]. HBZ also interacts with the p65 subunit of NF-κB, either preventing its DNA-binding activity or triggering it for degradation. [26]. HBZ is responsible for the activation of mTOR, a key regulatory inhibitor of the autophagy pathway[27,28]. Mice with transgenic *hbz* developed skin lesions early in their lifespan and 37% developed T-cell lymphomas after 1.5 years, demonstrating that *hbz* itself is able to predispose cells towards leukemogenesis. The same study found that transgenic *hbz*, and not transgenic *tax*, was responsible for effector/memory/regulatory T-cell proliferation [29]. In addition, in a comparison between ATLL, HAM/TSP, and asymptomatic HTLV-1 carriers, *hbz* mRNA was transcribed in every group while *tax* was not significantly transcribed [30]. Tax expression has been observed to be lost altogether in around 40-60% of ATLL cases, demonstrating that Tax is not always necessary to sustain ATLL [31–33]. This aligns with late stage ATLL, where sporadic switching on-and-off of Tax production can help prevent apoptosis, while consistent presence of HBZ in both forms prevents immune system activation through a shift towards proviral replication as a part of cell replication [4,25,34].

Extracellular Vesicles

Since its discovery, research into HTLV-1 has focused on the mediation of CD4+ T-cell malignancy. Only within the last decade has extracellular vesicles' role during viral infection begun to have been explored [35–38]. Extracellular vesicles (EVs) are membrane-bound vesicles excreted into the microenvironment by all domains of life—Bacteria, Archaea, and Eukarya [39]. When they were first discovered, they were believed to be merely be garbage disposal units for eukaryotic cells' unrecyclable components [40]. However, in recent years, EVs have been found to play an extensive role in cell-to-cell

communication by transporting a variety of cargo (lipids, proteins, and nucleic acids) from their donor cells to recipient cells [41,42].

EVs are heterogenous in size and in origin. Autophagosomes oftentimes can be precursors to multi-vesicular bodies (MVBs) or can fuse with lysosomes to degrade their contents; however, in a process called secretory autophagy, autophagosomes can also be directly exocytosed [43,44]. Apoptotic bodies (50 to over 1,000 nm) are a collective name for EVs released from cells undergoing apoptosis [45,46]. Ectosomeal microvesicles (typically 100-1,000 nm), bud off directly from the plasma membrane of cells and therefore tend to contain cargo that was present in the donor cell's cytoplasm [47,48]. Exosomes, typically 30-150 nm in size, are at the forefront of the field due to their small size range lending well towards isolation; they are formed via the endocytic pathway inside of multivesicular bodies (MVBs), which when exocytosed, release their exosomes into the extracellular space. Within the last few years, 39-71 nm non-membranous distinct nanoparticles or "exomeres" have been suggested as another EV subtype [49]. However, their recent discovery and questionable classification as "vesicles" prompts further confirmation into their origin and role.

Due to the wide size and density ranges of each EV subtype, and because many of these vesicles interact with the autophagy pathway, pure isolation is difficult to achieve. The predominant approach to enriching for specific subtypes involves differential ultracentrifugation, which involves sequential ultracentrifugation at higher r.c.f. /g-forces for longer periods of time to create subpopulations of EVs separated by density. For example, the 2K EV subpopulation refers to the EV pellet produced by spinning cell

supernatant at 2,000 × g for 45 minutes [50]. Canonically, the 2K subpopulation (2K) is enriched for autophagosomes and apoptotic bodies, the 10K for microvesicles, the 100K for exosomes, the 167K (4 hours) for small exosomes (sEVs), and the 167K (16 hours) for exomeres.[45,47,49,50]. However, extracellular vesicle studies outside of the 100K EV subpopulation are fairly recent and their contributions to the overall effects of EVs have not been as thoroughly examined yet.

Extracellular Vesicles and HTLV-1

Our lab has dedicated multiple studies to the intersection of HTLV-1 and extracellular vesicles. Exosomes from ATLL cells were found to contain Tax and HBZ protein and mRNAs and protect recipient cells from apoptosis [38]. These results were recapitulated in HAM/TSP PBMC exosomes. Tax protein was found within PBMCs and EVs isolated from HAM/TSP patient cerebrospinal fluid, where the supernatant was found to virus-free. Thus, EVs could be used to transport HTLV-1 proteins across the blood-brain barrier and result in HAM/TSP neurodegeneration.[51]. ATLL EVs were found to differ in cargo depending on their density after gradient ultracentrifugation. Denser ATLL EV fractions were found to contain mature gp46 envelope protein and a high amount of p19 matrix protein and HTLV-1 mRNAs, suggesting presence of viral particles or an abundance of mature viral components; however, these EVs were shown to be non-infectious. Less dense EV fractions still contained significant levels of HTLV-1 mRNAs, but instead held the unprocessed form of the envelope protein (gp61), suggesting the presence of free protein. ATLL EVs were also shown to promote cell-to-cell contact, increasing viral spread and integration into normally immune-privileged tissues [52]. A

recent study looking at 2K, 10K, and 100K ATLL EVs subpopulations recapitulated findings from the density gradient paper: the less dense 100K EVs contain less viral protein and induce a protective/growth effect upon recipient cells, dense 2K and 10K subpopulations contain the majority of viral proteins and induce deterioration of mesenchymal stem cells (MSCs)/aortic endothelial tubules similar to that of the blood-brain barrier[53].

Another recent paper involving ATLL EVs and MSCs found that the 100K EVs delivered Tax and microRNAs to MSCs, activating the NF-κB pathway and target genes. This resulted in proliferation and an increase in migration markers and VEGF, a pro-angiogenic molecule, and was attributed to helping aid in leukemic progression [54]. This phenotypic change is reminiscent of the effects that EVs from cancerous cells induce upon recipient, non-cancerous cells. The Nana-Sinkam lab found that metastatic lung cancer 100K EVs promote proliferation, epithelial-to-mesenchymal transition, migration, and invasion in human bronchial epithelial cells (HBECs) [55]. The Orth lab discovered that pancreatic cancer 100K EVs acted as initiators (damage inducers) but not promoters (selective proliferators) of neoplastic transformation in NIH-3T3 mouse fibroblasts[56]. The Krichevsky lab found that glioblastoma EVs aided in the proliferation of transformed astrocytes and fostered anchorage-independent growth in soft agar [57]. Because ATLL is a leukocytic cancer, ATLL EVs have the potential to interact with any cells that blood or biofluids interact with. However, a gap in knowledge exists relating to how ATLL EVs interact with differentiated non-leukocytes. In addition, because of a bias in the EV field towards the 100K / exosome subpopulation due to its narrow size range, many of the

conclusions made about the effects of "extracellular vesicles" may not hold for other subpopulations. Therefore, we approached this study with two aims in mind: first, to further characterize ATLL EV subpopulations with the addition of 167K (4hr) and 167K (16hr), and second, to analyze the effects of ATLL EV subpopulations upon recipient non-leukocytes, with an eye for hallmarks of cancer progression (e.g. immortalization, transformation, and migration/metastasis). We hypothesized that ATLL EVs may help push non-leukocytes forward in cancer progression. We expect that, because of the higher amount of Tax, the dense 2K and 10K EVs would help aid in anchorage-dependent growth. However, in a soft agar assay evaluating for migration, mesenchymal phenotype, and colony formation, we suspect that the less dense EVs (100K, 167K 4hr) would promote anchorage-independent growth.

MATERIALS AND METHODS

Cells and Reagents

The HTLV-infected human T lymphocyte cell line HuT102 (ATCC TIB-162.1) was cultured in RPMI-1640 (Quality Biological) complete media and the uninfected human cervix adenocarcinoma cell line HeLa (ATCC CCL-2) was cultured in DMEM (Quality Biological) complete media, both at 37°C with 5% CO_2. "Complete media" refers to the base media supplemented with 1% L-glutamine, 1% Penicillin-Streptomycin, and 10% exosome-free fetal bovine serum (FBS); exosome-free FBS was obtained through ultracentrifuging heat-inactivated FBS (Peak Serum) at 100,000 × g for 90 minutes to remove bovine EVs.

EV Isolation and Characterization

HuT102 cells were grown for 4 days in T225 flasks at 500mL with 0.018 ug/mL of IL-2. To produce HuT102 EV subpopulations, a process called differential ultracentrifugation was utilized: 180mL of cell suspension were centrifuged on a desktop centrifuge at 300 x g for 10 minutes to pellet cells and cell debris. The resulting supernatant was decanted into new tubes and ultracentrifuged in Beckman Ti70 rotor at 2,000 × g for 45 minutes, producing a "2K" EV pellet. This process was repeated with the same supernatant in new tubes at 10,000 × g for 45 minutes, 100,000 × g for 90 minutes, 167,000 × g for 4 hours, and 167,000 × g for 16 hours, resulting in the "10K", "100K", "167K (4hr)", and "167K (16hr)" EV subpopulation pellets, respectively. The 2K and 10K pellets were washed with 1 mL of 1x-Phosphate Buffered Saline (PBS) and repelleted, and all

pellets were resuspended with around 200 μL of PBS before being stored at −20°C. Average EV subpopulation concentration and size was characterized using ZetaView® Z-NTA (Particle Metrix).

Western Blot

A 5 μL aliquot of each EV subpopulation was processed with 15uL of Laemmli Buffer and loaded onto a 4-20% Tris-glycine gel (Invitrogen) and run at 180 V. Proteins were transferred to an Immobilon-P Transfer Membrane (Millipore) overnight at 50 mA. The resulting membrane was blocked with a 10 mL of a 5% powdered milk in PBS + 0.1% Tween 20 (PBS-T) mixture for 30 minutes at 4°C. After washing with PBS-T, a primary antibody was incubated on the membrane overnight at 4°C. Antibodies included α-p19 (Santa Cruz Biotechnology, sc-1665), α-gp61/46 (NIH AIDS Reagent Program Cat. #1578), α-Tax (cocktail of monoclonal mouse Tax antibodies 169, 170, and 171, a generous gift from Dr. Scott Gitlin, University of Michigan)[52,53], α-LC3B (Cell Signaling, Cat. #2775), α-CD81 (Systems Biosciences, Cat. # EXOAB-CD81A-1), α-CD9 (Systems Biosciences, Cat. # EXOAB-CD9A-1), α-CD63 (Systems Biosciences, Cat. # EXOAB-CD63A-1), α-Flotilin-1 (Santa Cruz Biotechnology, sc-74566), α-HSP90 α/β (Santa Cruz Biotechnology, sc-13119), α-GAPDH (Santa Cruz Biotechnology, sc-48166), and α-Actin (Abcam, ab49900).

After washing three times with PBS-T, the membrane was incubated with an HRP-conjugated secondary antibody for 2 hours at 4°C. Membranes were then washed twice with PBS-T and once with PBS before developing. Membranes were visualized using the

ChemiDoc Touch System (Bio-Rad) using the Clarity and Clarity Max Western ECL Substrates (Bio-Rad).

RNA Isolation and RT-qPCR

Total RNA was isolated from 10uL of each HuT102 subpopulation using TRIzol reagent (Invitrogen) and chloroform according to the manufacturer's protocol. RNA was quantitated using a NanoDrop 1000 spectrophotometer (ThermoScientific) and cDNA was generated using GoScript Reverse Transcription System and Oligo(dT)15 (Promega). RT-qPCR was then performed with 7uL of undiluted cDNA, SYBR green master mix (Bio-Rad), and the following primers: Fujisawa Tax-F (5' ATC CCG TGG AGA CTC CTC AA-3', T_m = 57.6°C); Fujisawa Tax-R (5' AAC ACG TAG ACT GGG TAT CC-3', T_m = 53.6°C); Fujisawa HBZ-F (5' AGA ACG CGA CTC AAC CGG-3', T_m = 57.8°C); Fujisawa HBZ-R (5' TGA CAC AGG CAA GCA TCG-3', T_m = 55.7°C). Reactions were carried out in triplicate on a BioRad CFX96 Real Time System. Analysis of data was carried out using Microsoft Excel.

Cell Viability Assay and Cell Proliferation Assay

On Day 0, HeLa cells grown at 70% confluency were plated in three 96-well plates at a density of $5 \cdot 10^3$ cells/well in 100 μL DMEM and treated with HuT102 EV subpopulations at a ratio of 1:1000 cells:EVs. Each treatment lane was performed in triplicate for use in the Cell Viability Assay, and two wells for cell counting were added as well, for a total of 5 wells per treatment per plate. On Day 2, one of the plates (the "Day 2 plate") was imaged at 20x magnification using an Invitrogen™ EVOS™ FL Auto Imaging System before being processed for use in assays. The two "cell counting wells" were

trypsinized and measured for average count using a hemocytometer. The three "Cell Viability wells" were measured by addition of CellTiterGlo Luminescence Viability Kit (Promega) according to the manufacturer's protocol before detecting luminescence with the GloMax Explorer multidetection system (Promega). On Day 2, the "Day 4" and "Day 6" plates received an additional EV subpopulation treatment at the same ratio. On Day 4, the "Day 4" plate was processed for Cell Viability and Cell Proliferation as was performed on Day 2, while the "Day 6" plate was given a third EV subpopulation treatment. On Day 6, the "Day 6" plate was processed for Cell Viability and Cell Proliferation, as was performed on Days 2 and 4.

Soft Agar Colony Formation Assay

This assay was modified from an existing protocol[58]. On Day -6, HeLa cells grown at 70% confluency were plated in 24-well plates at a density of $10 \cdot 10^4$ cells/well and treated with HuT102 EV subpopulations at a ratio of 1:1000 cells:EVs. On Day -3, the wells were given a 2nd treatment of HuT102 EV subpopulations at the same ratio. On Day 0, 6-well tissue culture plates were plated with 1.5 mL 1% "Bottom Agar" (750 µL 2% agarose in PBS + 750uL DMEM) per well and allowed to cool for 30 minutes. The HeLa cells from each treatment were trypsinized and resuspended in 750 µL complete DMEM; each cell suspension was mixed with 750 µL 0.6% agarose in PBS, resulting in 0.3% "Top Agar". 1.5mL of the 0.3% Top Agar was plated on top of the solidified "Bottom Agar" in its corresponding well; each treatment was plated in duplicate and topped with 1mL DMEM once solidified. Plates were incubated at 37°C with 5% CO_2 for 28 days, changing the media every 3 days. On Day 28, the plates were washed with 1x PBS and .5mL of

.005% aqueous Crystal Violet solution (Ward's Science) was incubated with each dish for 30 minutes before de-staining with diH_2O. Wells were then imaged at 20x magnification using an Invitrogen™ EVOS™ FL Auto Imaging System. Images were taken at five positions in each well, at two focal depths per position. For each position, blue colonies greater than 50 μm (as measured with ImageJ) were measured and counted, disregarding any duplicates between the two focal depths.

Statistical Analysis

Standard deviations of the data were calculated using Microsoft Excel. Student's two-tailed T test was utilized to calculate p-values. Statistical significance was denoted on the graphs per the following: * = $p < 0.05$, ** = $p < 0.01$, and *** = $p < 0.001$.

RESULTS

HuT102 EV subpopulations differ in HTLV-1 marker protein and RNA concentration

In our previous work, we showed that EVs from HTLV-1 transformed adult T-cell leukemia/lymphoma (ATLL) cells increased cell-to-cell contact and increased HTLV-1 viral spread [52,53]. Upon noticing that the effects of 100K ATLL EVs on recipient MSCs (increased proliferation, NF-κB activation, increased migration markers) resembled those of various tumors' EVs on recipient cells, we wondered if ATLL EVs may be acting like tumor EVs in modulating recipient cells more towards a neoplastic phenotype [54–57]. The aim of this study was to better understand the different impacts of individual ATLL EV subpopulations upon non-leukocytic cells. We hypothesized that ATLL EVs may help push non-leukocytes forward in cancer progression, with the denser EV subpopulations (2K, 10K) aiding in in proliferation due to presence of Tax and the less dense EV subpopulations (100K, 167K 4hr) promoting long term growth and phenotypic changes in recipient cells. To assess the validity of this hypothesis, we isolated EV subpopulations (2K, 10K, 100K, 167K (4hrs), and 167K (16hrs)) from the ATLL cell line HuT102 via differential ultracentrifugation **(Figure 1a)**. This was followed by a Western blot to assay for the distribution of HTLV-1, EV, and cellular markers within HuT102 EV subpopulations **(Figure 1b)**. Results show that HTLV-1 matrix protein p19, the processed form (gp46) of the HTLV-1 envelope protein, and the HTLV-1 transactivating oncoprotein Tax were concentrated in 2K and 10K EVs, with a slight presence in 100K EVs. No viral proteins

were found in 167K (4hr) or 167K (16hr) EVs. This finding correlates with the presence of autophagy markers LC3 I and LC3 II, with strong bands in the 2K and 10K, weaker bands in the 100K, and very weak bands in the 167K (4hr) and (16hr) subpopulations. Looking at EV markers, the tetraspanins CD81, CD9, and CD63 differed in distribution. CD81 showed faint bands in 100K and 167K (4hr) EVs, CD9 showed strong bands in 100K and 167K (4hr) EVs and a weak band in 167K (16hr) EVs, and only the glycosylated form of CD63 was present in our EVs, but across all EV subpopulations, with slightly elevated presence in 10K and 100K EVs. Flotillin, a protein that is involved with vesicle trafficking, showed bands in 10K and 100K EVs with weaker bands in 2K and 167K (4hr) EVs. HSP90, a heat shock protein typically associated with the cytoplasm, showed presence in 10K EVs, with weak presence in 2K and 100K EVs. GAPDH, a glycolysis enzyme typically used as a Western Blot cellular housekeeping marker, showed equally strong bands in 2K, 10K, and 100K EVs. Actin, a cytoskeletal protein also typically used as a Western Blot housekeeping marker, showed bands in 2K and 10K EVs and a weaker band in 100K EVs. Altogether, the 2K subpopulation showed strong presence of HTLV-1 markers and weak presence of EV markers, the 10K subpopulation showed strong presence of viral markers and EV markers, the 100K subpopulation showed weak presence of viral markers and strong presence of EV markers, the 167K (4hr) subpopulation showed an absence of viral markers and strong presence of EV markers, and the 167K (16hr) showed an absence of viral markers and weak presence of EV markers.

Next, we sought out to characterize the amounts of oncogenic mRNAs in HuT102 EV subpopulations. We isolated total RNA from each EV subpopulation and performed

RT-qPCR. The results in **Figure 1c** show that all EV subpopulations contain significant levels of *tax* and *hbz*, with an average copy number of $7.49 \cdot 10^3$ and $1.04 \cdot 10^8$ per 10uL of EVs, respectively. In both cases, the 2K EVs contained the most mRNA, while the 10K, 100K, and 167K (4hr) EVs contained significantly less mRNA. The 167K (16hr) for both genes had the significantly least mRNA, approximately 1 and 2 logs less than the 2K EVs, respectively. Altogether, the denser HuT102 EV subpopulations (2K and 10K) contain more HTLV-1 proteins and mRNAs than the less dense subpopulations (100K, 167K (4hr) and 167K (16hr)), but the less dense EVs contain more EV markers and a still significant amount of *tax* / *hbz* mRNA.

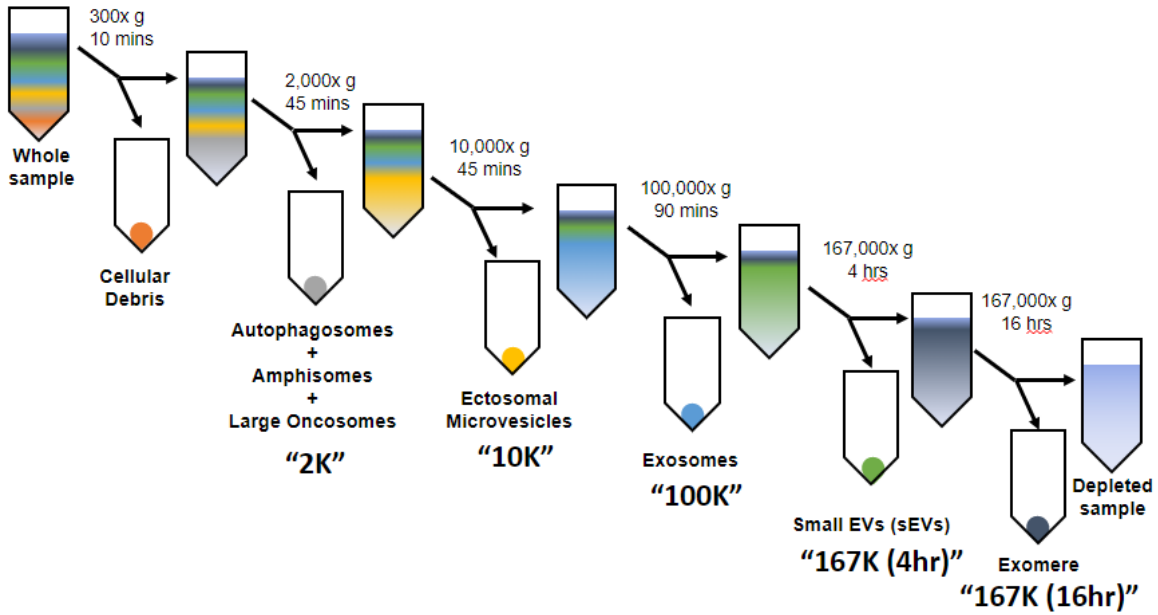

Figure 1a: Separation of Extracellular Vesicle Subpopulations using Differential Ultracentrifugation. HuT102 cell suspension was centrifuged on a desktop centrifuge at 300 x g for 10 minutes to pellet cells and cell debris. The resulting supernatant was decanted into new tubes and ultracentrifuged in Beckman Ti70 rotor at 2,000 × g for 45 minutes, producing a "2K" EV pellet. This process was repeated with the same supernatant in new tubes at 10,000 × g for 45 minutes, 100,000 × g for 90 minutes, 167,000 × g for 4 hours, and 167,000 × g for 16 hours, resulting in the "10K", "100K", "167K (4hr)", and "167K (16hr)" EV subpopulation pellets, respectively. The 2K and 10K pellets were washed with 1 mL of 1x-Phosphate Buffered Saline (PBS) and repelleted, and all pellets were resuspended with around 200 µL of PBS before being stored at −20°C.

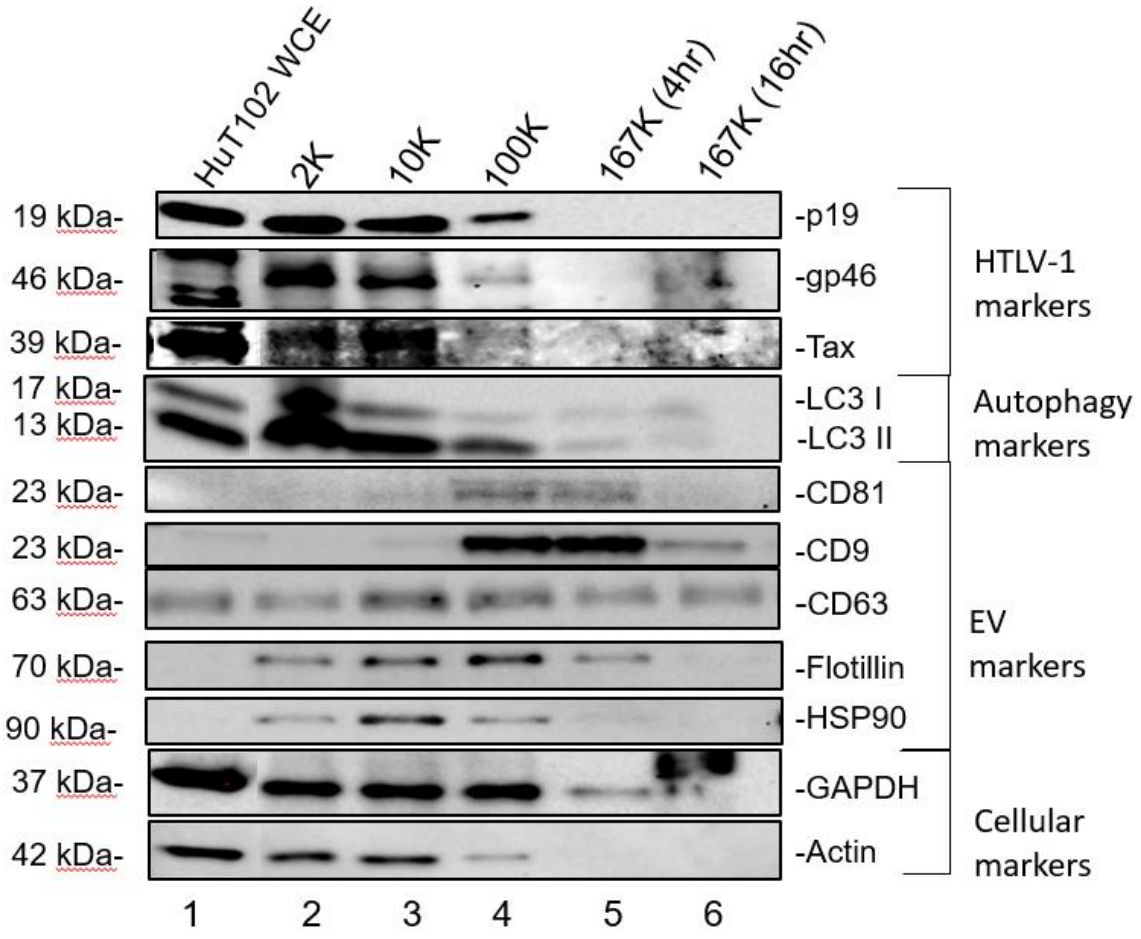

Figure 1b: Viral and EV Markers are distributed differently across HuT102 EV subpopulations. Differential ultracentrifugation was performed on 180 mL of cell supernatant from HuT102 cells to produce the 2K, 10K, 100K, 167K for 4 hours (167K 4hr), and 167K for 16 hours (167K 16hr).
A Western Blot was performed using EV subpopulations to characterize the presence of HTLV-1 markers (p19, gp46, and Tax), Autophagy marker (LC3 I/II) and EV markers (tetraspanins CD81, CD9, and CD63; vesicle trafficking marker Flotillin; and cytosolic chaperone protein HSP90). HuT102 Whole Cell Extract (WCE) was used as a positive control for HTLV-1 markers. GAPDH and actin were used as cellular housekeeping markers.

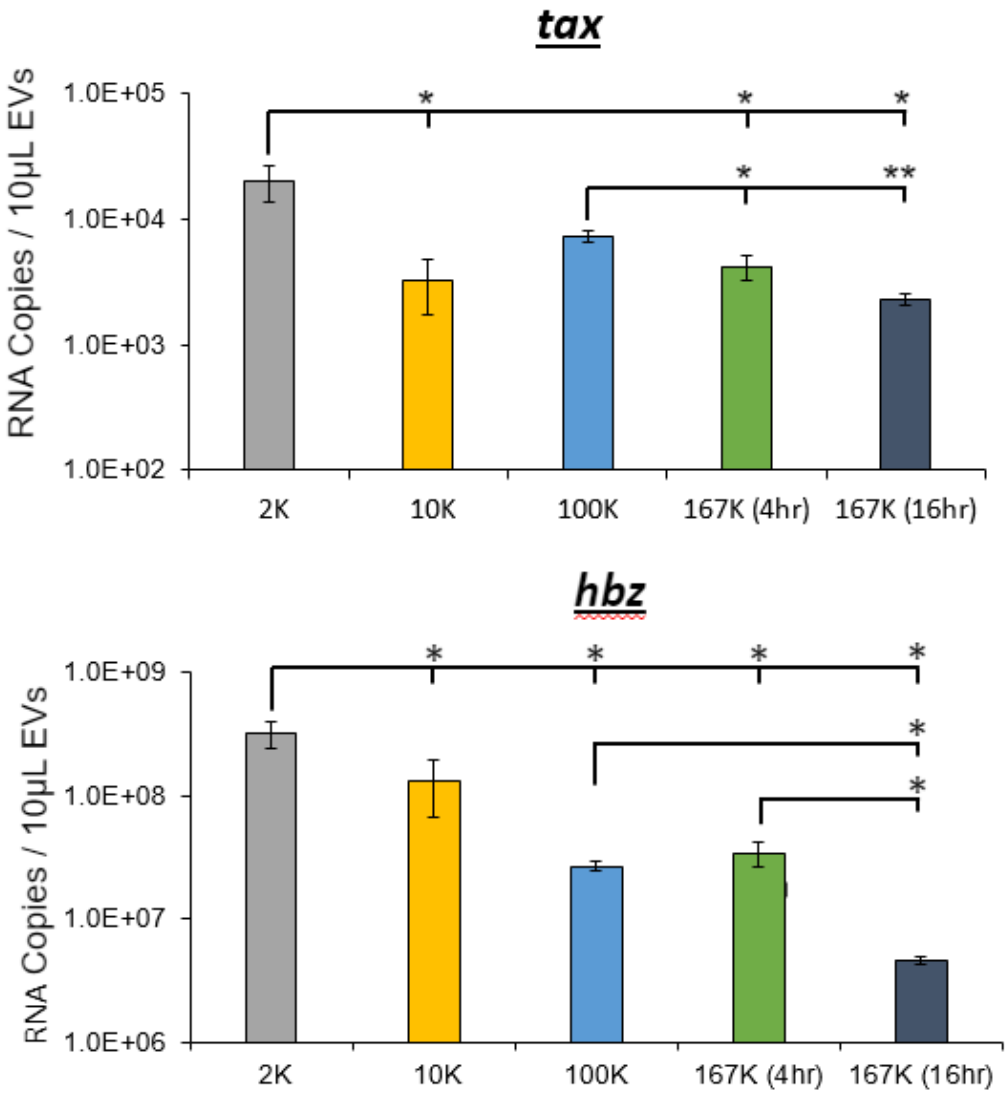

Figure 1c: HTLV-1 oncogene mRNA transcripts are present in all HuT102 EV subpopulations.
Differential ultracentrifugation EV subpopulations (2K, 10K, 100K, 167K (4hr), and 167K (16hr)) were prepped for RNA isolation and RT-qPCR for HTLV-1 *tax* levels and HTLV-1 *hbz* levels. Error bars represent one standard deviation from the mean. Student's two-tailed T test was utilized to calculate p-values. Statistical significance was denoted on the graphs per the following: ***** = $p < 0.05$, ** = $p < 0.01$.

HuT102 EV subpopulations exert differential effects on phenotype in post-confluent HeLa cells and promote HeLa cell proliferation.

Next, we asked whether HuT102 EV subpopulations would differ in their ability to induce proliferation in recipient cancer cells. As shown in **Figure 2a**, recipient HeLa cells were treated with HuT102 EV subpopulations once (for the Day 2 plate), twice (for the Day 4 plate), or thrice (for the Day 6 plate) before taking images of the wells (**Sup. Fig. 1a, Sup. Fig. 1b, Figure 2b,** respectively) and analyzing either for Cell Viability by quantifying ATP (**Sup. Fig. 2**) or for Anchorage-Dependent Proliferation using a hemocytometer (**Sup. Fig 3**, **Figures 2c**). Taking a look at **Figure 2b**, at Day 6, cells have reached post-confluency and were experiencing more acidic and nutrient-depleted media. Looking at the untreated 'HeLa Alone' well, we see a variety of abnormal cells phenotypes in addition to the healthy "cobblestone" phenotype (see **Sup. Fig. 1b)**. Comparing across EV subpopulation treated wells, EV treatment seems to have reduced the proportion and severity of the abnormal phenotypes, apart from 167K (4hr), which saw an increase in the clumping phenotype. **Supplemental Figures 1a** and **1b** also show the beginnings of this tight clumping in the 167K (4hr) well on Days 2 and 4.

After images were taken of wells, some of them were utilized for a Cell Viability assay (**Sup. Fig. 2**). All treated wells increased in ATP significantly from Day 2 to Day 4, however no significant difference occurred between the control and treated wells nor between EV subpopulation treatments. No significant difference was found between Day 4 and Day 6 either. Turning to the Cell Proliferation assay, **Supplemental Figure 3**

displays the data plotted by day. No significance is seen on Day 2, but on Day 4, the 10K, 100K, and 167K (4hr) EV subpopulations are significantly less than the 2K or 167K (16hr) EV treatments. However, at Day 6, the inverse occurred, as the 10K and 100K EVs were significantly higher than the HeLa Alone and 167K (16hr) treatments. Replotting this data looking within each EV subpopulation treatment (**Figure 2c**) fleshes out an interesting pattern: the HeLa Alone control and the 2K and 167K (16hr) treatments share a similar pattern of steady growth. However, in the 10K, 100K, and 167K (4hr) wells, we see another growth pattern: a lag from Day 2 to Day 4 before a boom in proliferation between Days 4 and 6. Altogether, this data demonstrates that although all HuT102 EV subpopulations did not have a huge effect on viability, and for the most part reduced abnormal morphologies in post-confluent cells, EVs subpopulations differ in their abilities to promote cell proliferation

A)

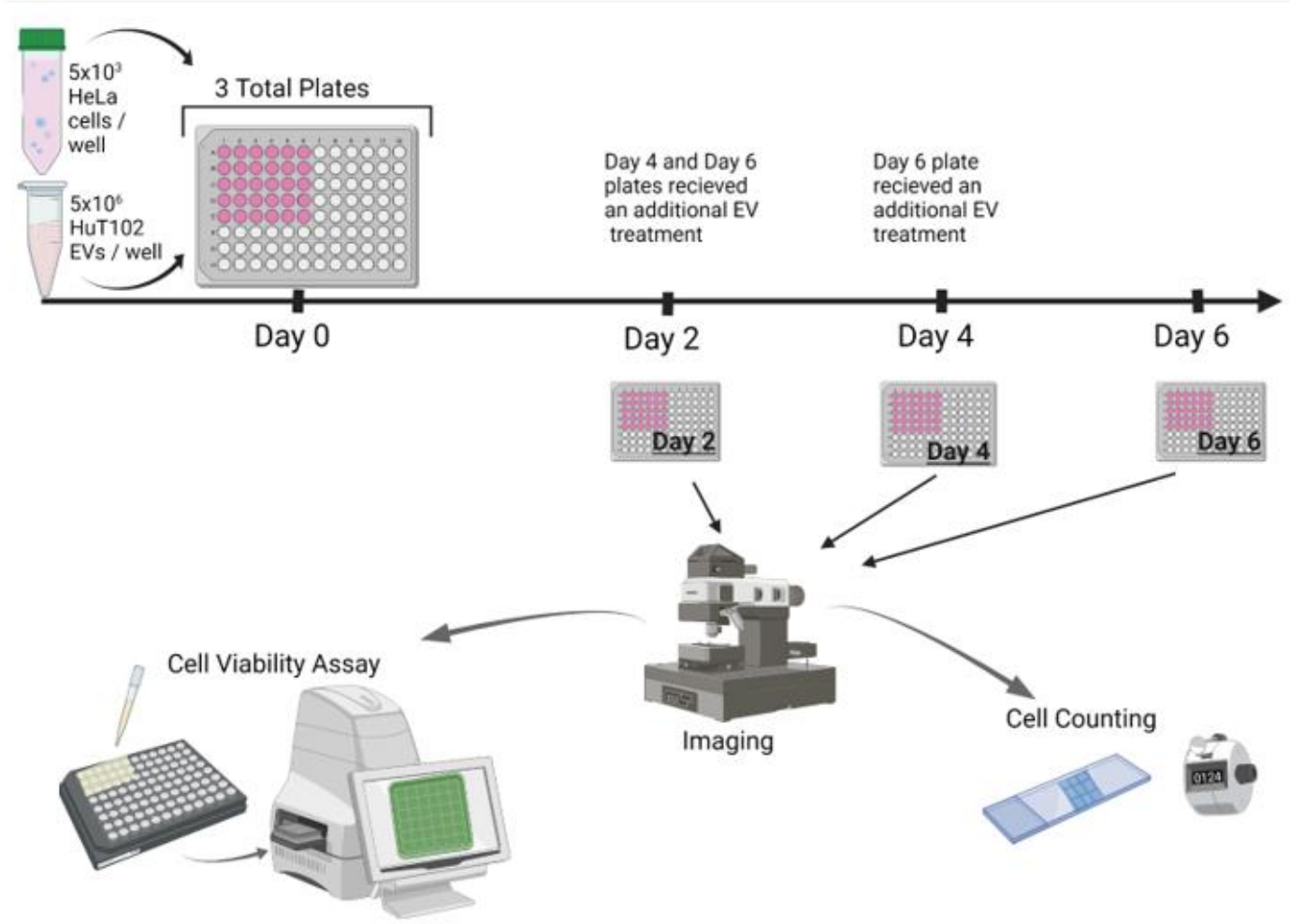
5x10³ HeLa cells / well
5x10⁶ HuT102 EVs / well
3 Total Plates
Day 4 and Day 6 plates recieved an additional EV treatment
Day 6 plate recieved an additional EV treatment
Day 0
Day 2
Day 4
Day 6
Day 2
Day 4
Day 6
Cell Viability Assay
Imaging
Cell Counting

B)

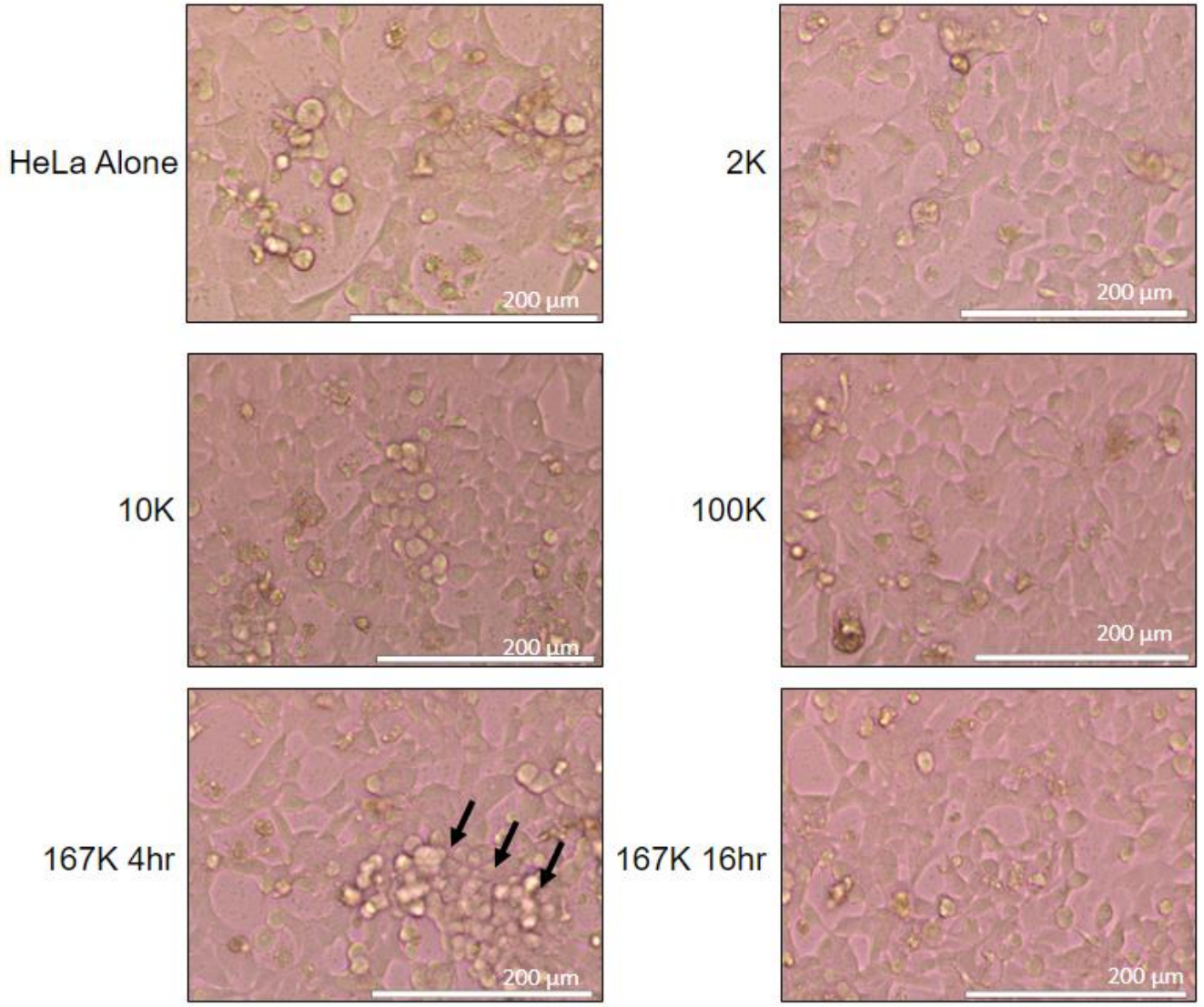
HeLa Alone
200 µm
2K
200 µm
10K
200 µm
100K
200 µm
167K 4hr
200 µm
167K 16hr
200 µm

C)

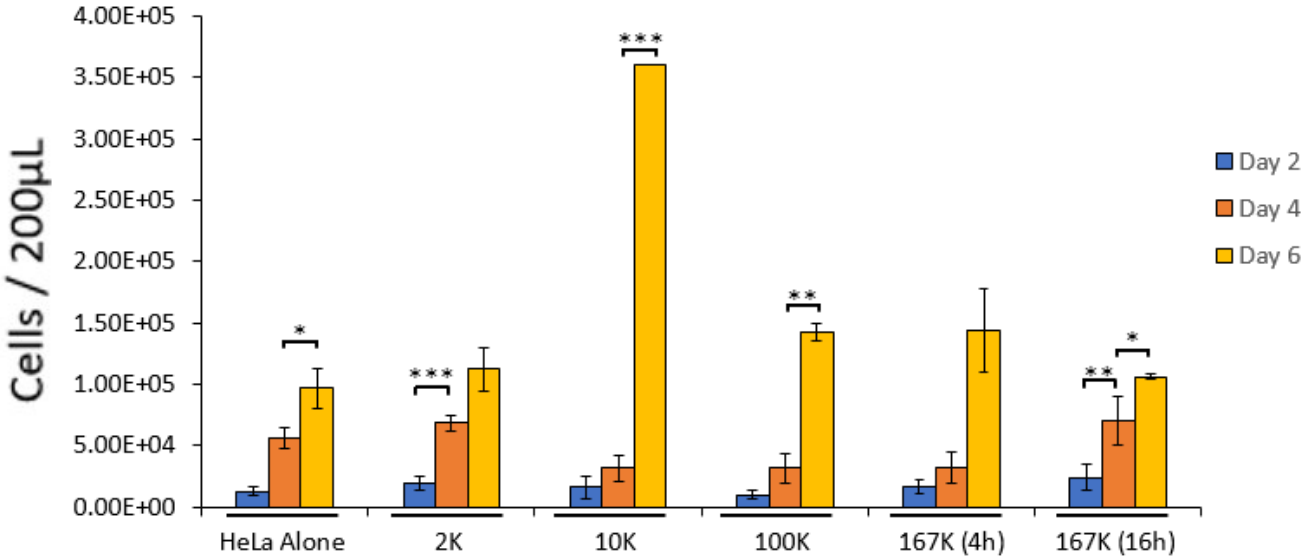

Figure 2: HuT102 EV subpopulations differentially promote HeLa cell proliferation and changes in morphology. a) Diagram of experimental design for preparing HuT102 EV subpopulation treated cells for subsequent experiments. HeLa cells were treated in a 96-well plate with either 1x-PBS (HeLa Alone) or with EV subpopulations at a 1:1000 (recipient cell : EVs) ratio every 2 days for 6 days. **b)** Wells were imaged at 20x using an Invitrogen™ EVOS™ FL Auto Imaging System on Day 6. Arrows indicate clumping phenotype. Scale bar is 200 µm. **c**) For the anchorage-dependent growth assay, cells were trypsinized and counted using a hemocytometer. Error bars represent one standard deviation from the mean. Student's two-tailed T test was utilized to calculate p-values. Statistical significance was denoted on the graphs per the following: * = $p < 0.05$, ** = $p < 0.01$, *** = $p < 0.00$

Less dense HuT102 EV subpopulations encourage HeLa cell anchorage-independent growth

Finally, we asked whether HuT102 EV subpopulations would encourage anchorage-independent growth similarly to anchorage-dependent growth in the Cell Proliferation Assay. **Figure 3a** outlines the process through which the Soft Agar assay was conducted. **Figure 3b** shows the number of colonies counted at each position within the treatment wells, with the bar representing the average number of colonies. The 2K, 10K, and 167K (4hr) treatments showed little difference in colony formation to the untreated HeLa Alone control. However, the However, the 100K, and 167K (16hr) treated wells showed more consistent anchorage-independent growth. Altogether, these less dense EVs promote HeLa cell anchorage-independent growth in a Soft Agar colony assay system.

A)

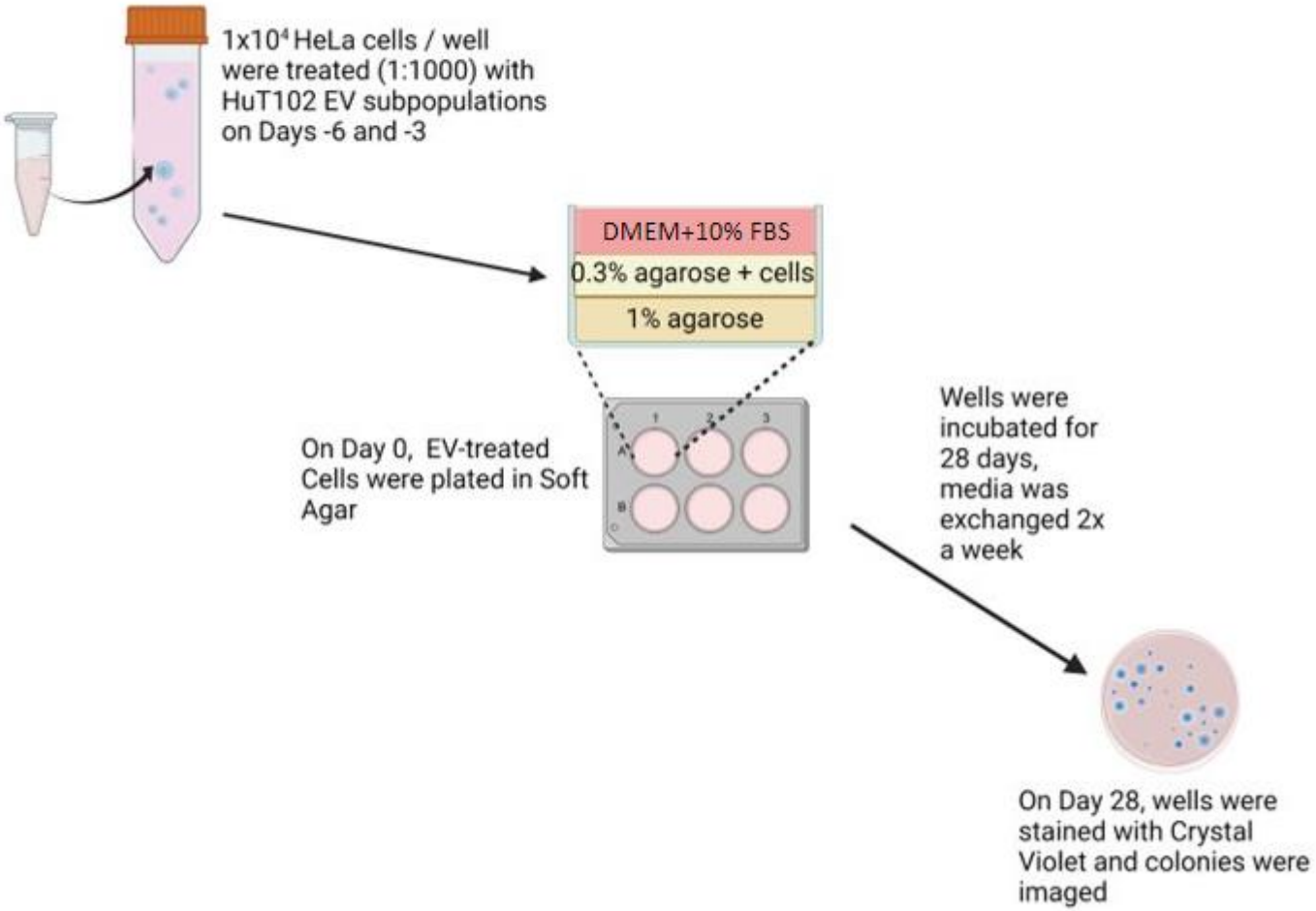
1x10⁴ HeLa cells / well were treated (1:1000) with HuT102 EV subpopulations on Days -6 and -3
DMEM+10% FBS
0.3% agarose + cells
1% agarose
On Day 0, EV-treated Cells were plated in Soft Agar
Wells were incubated for 28 days, media was exchanged 2x a week
On Day 28, wells were stained with Crystal Violet and colonies were imaged

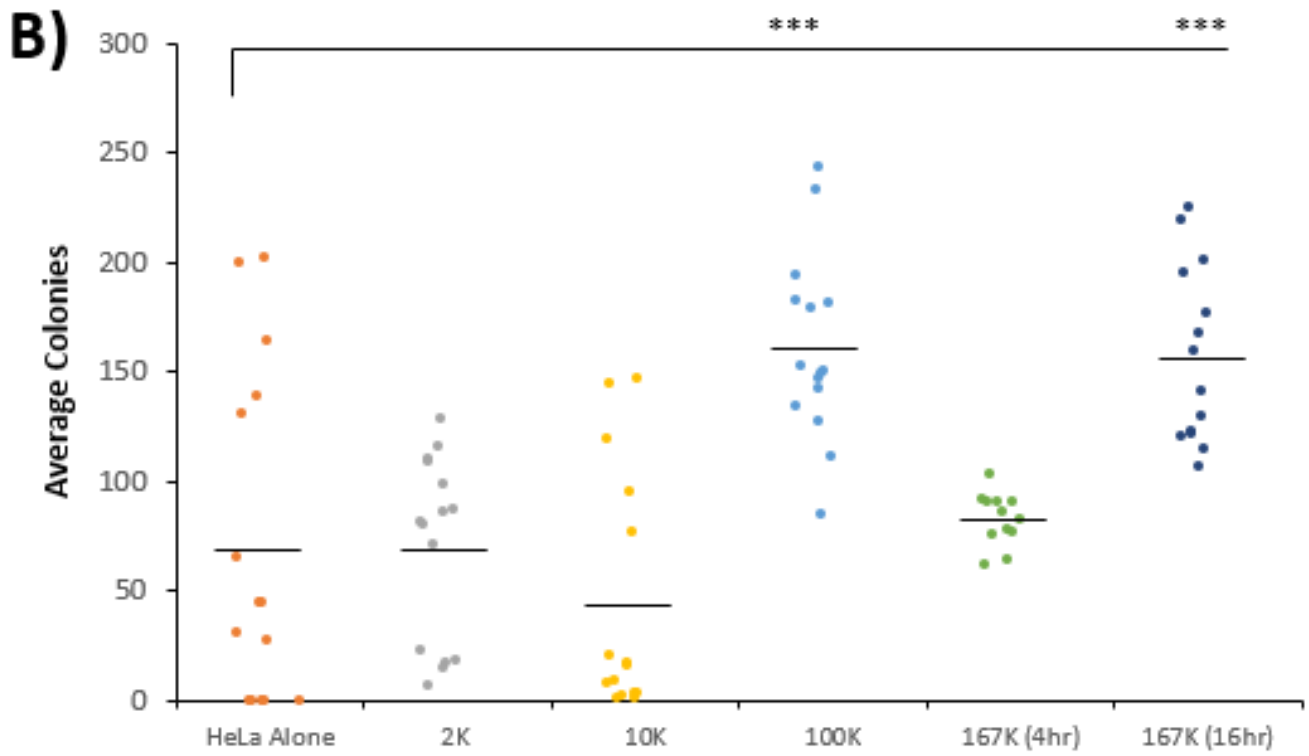

Figure 3: HuT102 100K and 167K (16hr) EV subpopulations encourage anchorage-independent growth in HeLa cells. a) Figure demonstrates the process of preparing the Soft Agar colony formation assay. HeLa cells were treated in a 24-well plate with either 1x-PBS (HeLa Alone) or with EV subpopulations at a 1:1000 ratio every 3 days for 6 days. Cells were trypsinized, resuspended in DMEM + 10% FBS, and mixed 1:1 with 0.6% agarose to create a 0.3% agarose + cells mixture. Seeded agarose was plated on a 1% agarose layer in 6-well plates and covered with 1mL DMEM + 10% FBS. Plates were incubated for 28 days, changing the media every 3.5 days. **b)** At 28 days, cells were washed and stained with .005% aqueous Crystal Violet solution before imaging. Stained colonies >50 μm (as measured using ImageJ) were counted. Three replicate experiments were performed, and each horizontal black bar represents an average count from all three wells. Student's two-tailed T test was utilized to calculate p-values. Statistical significance was denoted on the graphs per the following: ** = $p < 0.01$, *** = $p < 0.001$

DISCUSSION

The involvement of extracellular vesicles in promoting pathogenesis of viruses represent a recent shift in the EV field within the last 10-15 years[59]. Many viruses hijack portions of the autophagy pathway to either prevent the cell from interfering with proliferation or to allow a method of egress [44]. However, the effects of EVs from virally infected cells onto uninfected, recipient cells present a new angle to examine pathogenesis and disease formation. Previous studies from our lab and others demonstrate the capabilities for ATLL EVs to promote cell-to-cell contact and increase infection of recipient CD4+ T cells, and to promote proliferation, migration, and angiogenesis akin to cancer EVs.[52–54] This current study builds upon earlier findings, aiming to expand the scope to include the full range of HuT102 EV subpopulations (**Figure 1a**) and to non-leukocytic cells. Our findings indicate that HuT102 EV subpopulations impart differential effects upon recipient HeLa cells.

By performing a Western Blot using our EV subpopulations, we found that viral proteins, including the matrix protein p19, the mature envelope protein gp46, and the oncoprotein Tax were concentrated primarily within the 2K and 10K EV subpopulations **(Figure 1b)**. This aligns with our previous studies, where Tax and other viral proteins accumulated in the 18% (densest) density gradient ultracentrifugation fraction and in the 2K and 10K subpopulations. Historically, HuT102 EVs have been considered non-

infectious despite their viral protein and mRNA content [52]. This accumulation within the 2K and 10K could be in part due to Tax's downstream effects of increasing autophagosome production but preventing autophagosome/lysosome fusion, leading to an accumulation of autophagosomes with viral proteins [60]. This conclusion aligns with our findings that the uncleaved and cleaved forms of LC3, markers of autophagosome formation, also correlate with the 2K and 10K fractions. Another explanation is that some segment of these subpopulations are immature viral particles. 65-90% of free HTLV-1 virions have been observed to be deficient in or completely lack the capsid core structural protein, which is argued to make these viral particles non-infectious [61,62]. Both not-mutually-exclusive explanations would help to explain why the 2K and 10K seem to significantly promote cell-to-cell contact in recipient T-cells. The Western blot also confirmed that EV markers had more of an even distribution across the subpopulations, but most of the markers were concentrated in the 10K-167K (4hr) subpopulations. However, the presence of the glycosylated form of CD63, typically correlating with advanced HTLV-1 infection, has not been demonstrated previously outside of 18% density fraction nor outside of the 2K and 10K subpopulations. Collectively, this data demonstrates the heterogeneity of viral and EV protein distribution within HuT102 EV subpopulations and implies that each may impart differential effects onto recipient cells.

We then investigated the presence of viral mRNAs in HuT102 EV subpopulations. Although RT-qPCR of *tax* and *hbz* mRNA had been performed in our paper using density gradient ultracentrifugation, which demonstrated presence of both *tax* and *hbz* in all density fractions with a peak in the 18% (densest) fraction, it had not been performed in our

previous paper examining 2K, 10K, and 100K EV subpopulations from HuT102. Only *env* had been run via RT-qPCR, showing up in the 2K and 10K [52,53]. We hypothesized that we would see a similar pattern from the 2019 paper, with both mRNAs peaking in the dense 2K subpopulation but still showing presence at least until the 167K (4hr) subpopulation. After performing RT-qPCR (**Figure 1c**), the results confirmed that not only did both mRNAs show up throughout all subpopulations, peaking in the 2K and lowest in the 167K (16hr) EVs, but also that more *hbz* mRNA than *tax* was present, seeing almost a 4.5 log difference [52]. This result aligns with the ATTL model that *tax* is only periodically transcribed in the cells while *hbz* is always transcribed, thus leading to the gap of transcript numbers between the two [34,63]. Collectively, these results demonstrate that all HuT102 EV subpopulations, despite not all containing Tax protein, all contain both *tax* and *hbz* mRNA.

We then performed a series of assays (**Figure 2a**) using HuT102 EV subpopulations and the human cervix adenocarcinoma cell line HeLa to investigate what impact the subpopulations would have, if any, upon cancer cell morphology, viability, and proliferation. Exosomes / 100K EVs from ATLL had previously been shown to promote proliferation in mesenchymal stem cells, and other cancer exosomes have also increased cell proliferation[54,64]. Cells after Day 6 of EV subpopulation treatment showed that normal "cobblestone" phenotype was partially preserved by most subpopulations; however, the 167K (4hr) showed an increased presence of the clumping phenotype since Day 2 to Day 6 (**Figure 2b, Sup. Fig. 1a-b**). More research is necessary to understand what within the 167K (4hr) is inducing this phenotype, as it doesn't correlate to any factors

examined in this study. However, it might be due to EV uptake dynamics, as an unpublished fluorescent EV uptake assay from our lab found that, as opposed to autocrine uptake (HuT102 EVs placed on HuT102 cells) where 50% of cells had taken up the EVs by 24 hours, endocrine uptake (HuT102 EVs on 293T kidney cancer cells) did not see any EV subpopulation reach 50% uptake, even after 48 hours. The 167K (4hr) EV subpopulation was the first EV subpopulation to reach 40% uptake, however, and therefore either a favorable size or the mechanism of uptake might be the reason we see an increase in clumping in the 167K (4hr) treated HeLa cells. The Cell Viability assay (**Sup Fig. 2**) demonstrated no discernable impact of the addition of HuT102 EVs on HeLa cell viability, as opposed to previous experiments in our lab which showed that HuT102 cells require uptake of their own EVs to remain viable (data not shown). Prior experiments with a higher initial cell seeding density saw cell viability decrease at Day 4 while Cell Proliferation assays showed an increase over time (data not shown). This called to our attention that the CellTiterGlo assay is an ATP assay being used to infer about Cell Viability. However, this correlation is not absolute: cancer cells that reach confluency decrease in their ATP production despite continuing to proliferate [65]. Thus, great care needs to be taken to ensure that ATP production is not decreasing due to other factors if the CellTiterGlo is to be understood as a viability assay in the future. The Anchorage-Dependent Proliferation assay (**Sup. Fig. 3, Figure 2c**) demonstrated an interesting phenomenon, as at Day 4, HeLa cells treated with 10K, 100K, and 167K (4hr) EV subpopulations were significantly less proliferative than the control, 2K, or 167K (16hrs). However, the 10K, 100K, and 167K (4hr) EV subpopulations saw a boom in proliferation from Days 4 to 6, reversing the earlier

trend. This 2K and 167K (16hr) grouping also manifested in two experiments performed by our lab: an uptake assay with BODIPY-tagged HuT102 2K and 167K (16hr) subpopulation being taken up by HuT102 recipient cells 18 hours earlier than the other subpopulations, and as being the two most reparative subpopulations in a scratch assay with human bronchial epithelial cells (data not shown). This suggests that, if other cells uptake the 2K and 167K (16hr) EVs at a similar timeframe as HuT102 cells, that these EVs may have a head start in helping promote growth in recipient cells. However, this hypothesis needs to be further investigated, especially with uptake assays involving several different kinds of recipient cells. Collectively, these results demonstrated that although HuT102 EV subpopulations have no discernable impact on recipient HeLa cells' ATP production and generally all help preserve HeLa's natural morphology, the subpopulations fall into distinct groups which promote proliferation pre- and post-confluence.

Finally, we wanted to investigate whether HuT102 EV subpopulations would aid HeLa cells in anchorage-independent proliferation. Anchorage-independent growth is a key stage in cancer becoming metastatic and is a feature of epithelial-mesenchymal transition, which cancer exosomes have been reported to provoke [55,57,66,67]. After a 6-day co-culture period and then a 28-day soft agar culture (**Figure 3a**), 100K and 167K (16hr) subpopulation treated wells had a significant increase in the number of colonies as compared to the HeLa alone control well (**Figure 3b**). The 100K EV results lines up well with conventional EV literature wisdom on the 100K being reparative, however, the 167K (16hr) subpopulation is surprising, considering it didn't significantly assist in anchorage-dependent proliferation. Collectively, less dense EV subpopulations —100K EVs and

smaller—contribute towards anchorage-independent colony formation in HeLa cells. Optimization of the Soft Agar protocol, perhaps by transitioning the assay from being performed in 6-well plates to 24-well plates, will likely help tighten the variation seen in the 2K and 10K treated wells. In addition, additional ATTL cell line donor EVs and recipient epithelial cell types should be considered in order to make a generalizable statement on ATLL EVs' role in anchorage-independent growth.

Altogether, our earlier hypothesis about 2K and 10K potentially having an outstanding proliferative effect due to their Tax content seems to be incorrect. As summarized in **Table 1,** Anchorage-dependent growth seems to be the strongest in HuT102 subpopulations that possess high numbers of EV marker proteins (10K, 100K, 167K 4hrs), while anchorage-independent growth seems to be strongest in subpopulations without high amounts of viral protein content (100K, 167K (4hr), and 167K (16hrs). The 10K subpopulation could benefit anchorage-dependent proliferation by having sizable amounts of viral and vesicle proteins, while the 100K subpopulation has been the focus of most EV studies and is generally understood to have protective and proliferative effects[53,54]. However, the exact mechanism behind these differences is unknown and prompts further proteomics and nucleomics experiments to determine if the differing contents of these vesicles causes difference in recipient cell effects. Altogether, this data demonstrates the need for research into disease and cancer progression to expand beyond the 100K / exosome bubble, as these subpopulations are normally intermingled within body fluids but can have differing effects upon recipient non-leukocytes.

		2K	10K	100K	167K (4hr)	167K (16hr)
Characterization	Viral Proteins	+++	+++	+	+/-	+/-
	Autophagy Markers	+++	+++	++	+	+
	tax mRNA (~10^4)	+++	++	++	++	+
	hbz mRNA (~10^8)	+++	++	++	++	+
	EV Markers	+	++	+++	++	+
Recipient Cell Assays	Anchorage Independent Proliferation	+/-	+/-	++	+/-	++
	Anchorage-Dependent Proliferation	+/-	+++	+	+	+/-

Table 1: Summary of Experimental Trends. This table represents a summary of the trends from Characterization (Figures 1a-c) and Recipient Cell Assays (Figures 2 and 3).
"+++" refers to a result >75% from the baseline,
"++" refers to a result >50% from the baseline,
"+" refers to a result >25% from the baseline,
"+/-" refers to a result <25% from the baseline.

Future experiments based upon this data should try to address how does Tax and other HTLV-associated oncogenic markers in EVs influence cancer progression in leukocytes and non-leukocytes. In addition to refining the soft agar protocol, it would be prudent for future researchers to look at epithelial-to-mesenchymal transition markers like vimentin, n-cadherin, and tumor factor [54,55]. This could also be expanded to other aspects of cancer progression, like immortalization of primary cells and transformation of cell signaling. An example of such an experiment we want to run is shown in **Figure 4,** where primary T cells isolated from PBMCs would be incubated with EV subpopulations from HuT102, A549 (an adenocarcinoma epithelial cell line as another source of cancer EVs), and MSCs/IPSCs (to compare any proliferative effects of cancer EVs to stem cell EVs). In addition, our lab never tested a combined "All" treatment of EV subpopulations with these assays, so it would be interesting to see if a combined EV stock would allow for the recipient cells to reap the "early" proliferative benefits of the 2K and 10K while keeping the "late" proliferative benefits of the 100K, 167K (4hr), and 167K (16hr). One last area of further investigation would be cytokine production. ATLL cells have a noticeable shift in cytokine production upon transformation from primary CD4 T cells [68]. Our previous paper has examined ATLL EV-induced cytokine production in astrocytes, macrophages, mDCs, and neuroblasts[53], while another publication found that ATLL 100K EVs increased INF-γ in recipient PBMCs [69]. However, it would be interesting to see whether ATLL EVs cause a more generic cancer-cytokine upregulation in other types of non-leukocytic cells or whether an ATLL-specific cytokine profile is induced.

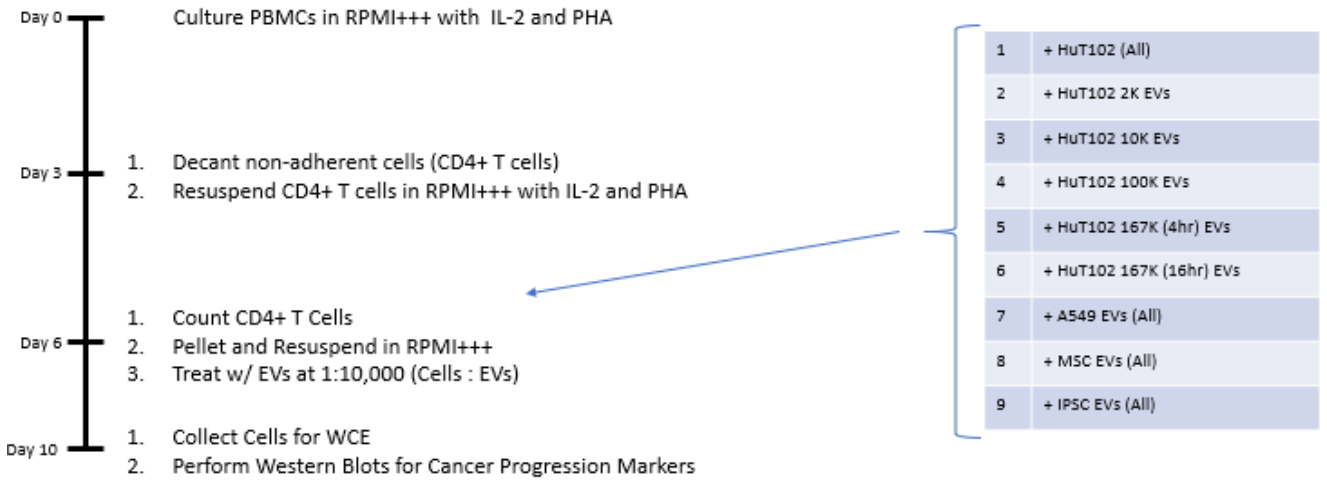

Figure 4: Experimental Design for Evaluating HuT102 EV subpopulations' effects on Cancer Progression in T-Cells: Figure represents the experimental design for an experiment to evaluate the effects of HuT102 EV subpopulations on various stages of cancer progression. RPMI+++ refers to RPMI-1680 media supplemented with Fetal Bovine Serum, L-glutamine, and Penicillin-Streptomycin. The "All" EV treatment refers to an equal volume mixture of each subpopulation. A549 is an adenocarcinoma epithelial cell line. MSCs are mesenchymal stem cells. IPSCs are Induced Pluripotent Stem Cells. P-p65 and P-AKT refers to phosphorylated versions of the p65 subunit of NF-κB and Akt (Protein Kinase B), respectively. Arrows refer to predicted increases or decreases in response to HuT102 EV treatment based on literature review.

SUPPLEMENTAL FIGURES

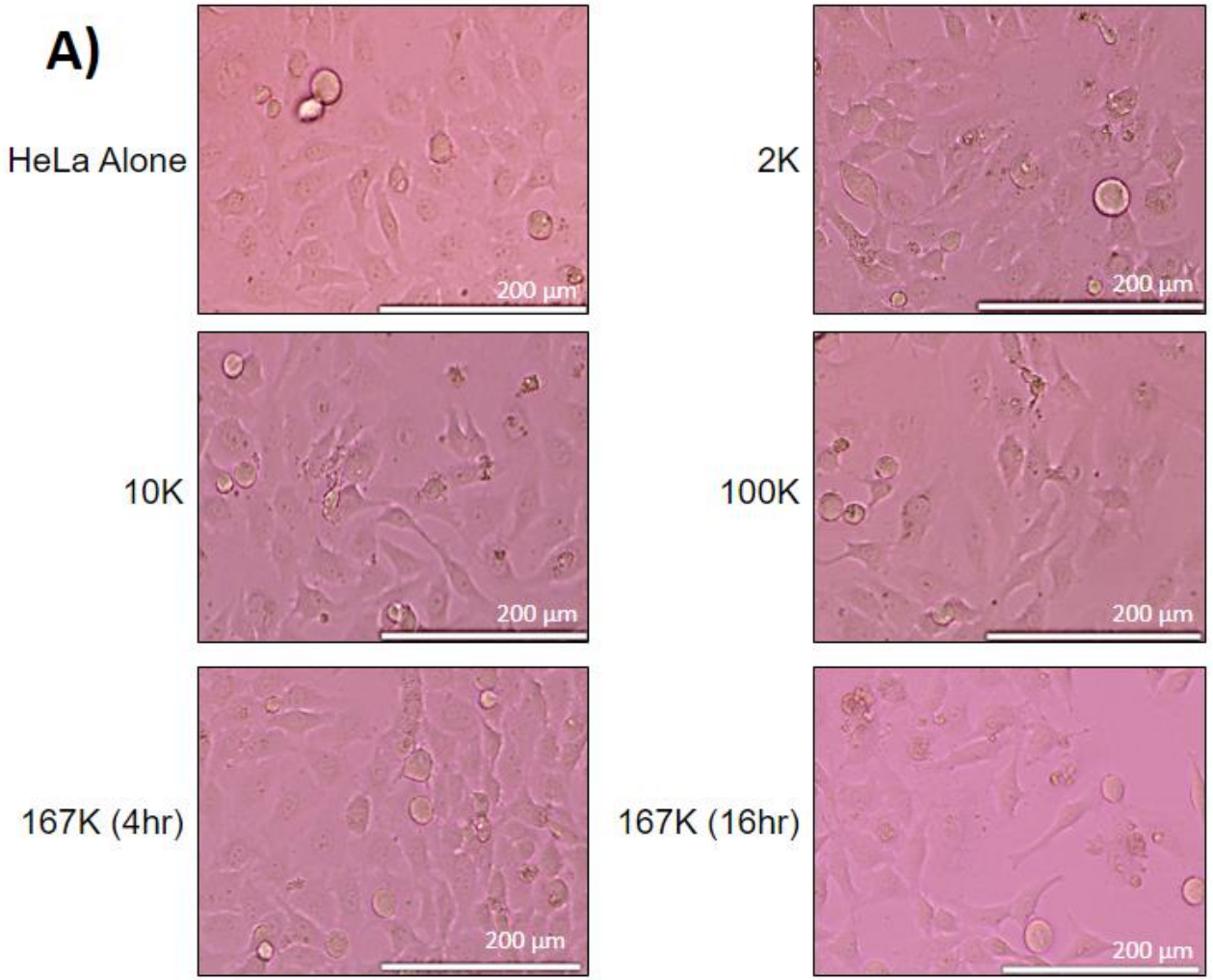
A)
HeLa Alone
2K
10K
100K
167K (4hr)
167K (16hr)
200 µm

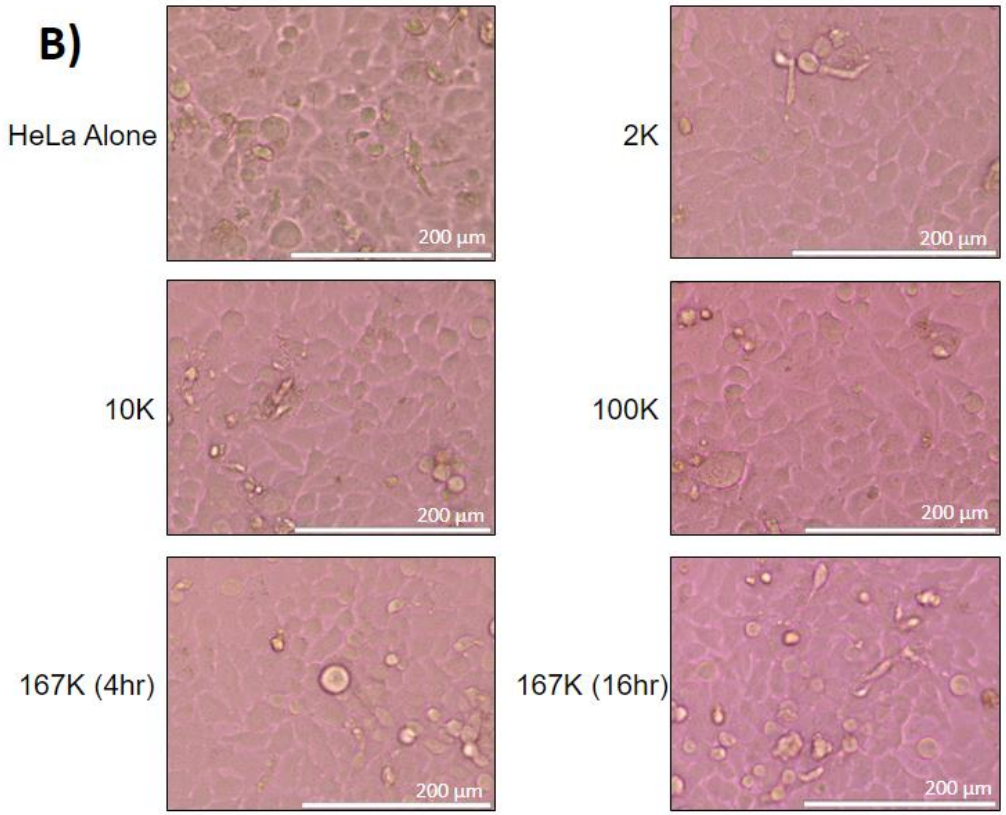

Supplemental Figure 1: HuT102 EV subpopulations' effects on phenotype in growing and in confluent HeLa cells. HeLa cells were treated in a 96-well plate with either 1x-PBS (HeLa Alone) or with EV subpopulations at a 1:1000 (recipient cell : EVs) ratio every 2 days for 6 days. Wells were imaged at 20x using an Invitrogen™ EVOS™ FL Auto Imaging System. Images show **a)** Day 2 and **b)** Day 4. Scale bar is 200 µm.

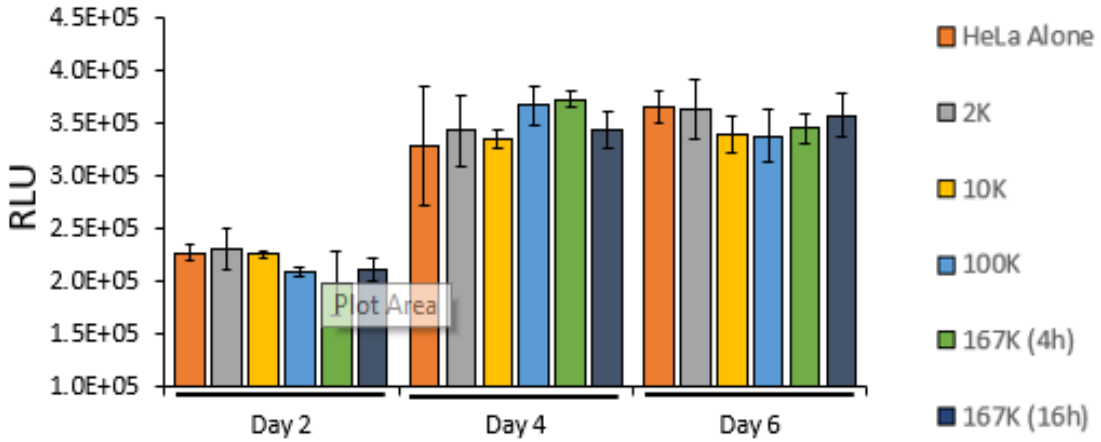

Supplemental Figure 2: Effects of HuT102 EV subpopulations on cell viability. HeLa cells were treated in a 96-well plate with either 1x-PBS (HeLa Alone) or with EV subpopulations at a 1:1000 (recipient cell : EVs) ratio every 2 days for 6 days. Cells were incubated with CellTiterGlo kit (Promega) before using a GloMax explorer to detect luminescence. RLU = relative light units.

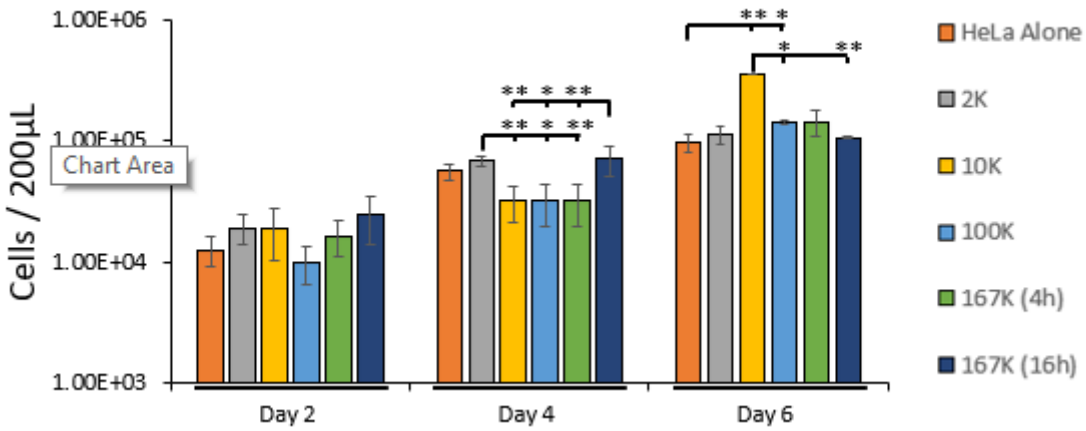

Supplemental Figure 3: Alternate graphing of Anchorage-Dependent Growth Assay. HeLa cells were treated in a 96-well plate with either 1x-PBS (HeLa Alone) or with EV subpopulations at a 1:1000 (recipient cell : EVs) ratio every 2 days for 6 days (Promega). Cells were trypsinized and counted using a hemocytometer Instead of grouping the data by treatment type as in Figure 2c, this graph groups the data by day of treatment. Error bars represent one standard deviation from the mean. Student's two-tailed T test was utilized to calculate p-values. Statistical significance was denoted on the graphs per the following: * = $p < 0.05$, ** = $p < 0.01$

REFERENCES

1. Poiesz BJ, Ruscetti FW, Gazdar AF, Bunn PA, Minna JD, Gallo RC. Detection and isolation of type C retrovirus particles from fresh and cultured lymphocytes of a patient with cutaneous T-cell lymphoma. Proceedings of the National Academy of Sciences. 1980; 77(12):7415–7419. doi:10.1073/pnas.77.12.7415.

2. Barré-Sinoussi F, Chermann J, Rey F, Nugeyre M, Chamaret S, Gruest J, et al. Isolation of a T-lymphotropic retrovirus from a patient at risk for acquired immune deficiency syndrome (AIDS). Science. 1983; doi:10.1126/SCIENCE.6189183.

3. Proietti FA, Carneiro-Proietti ABF, Catalan-Soares BC, Murphy EL. Global epidemiology of HTLV-I infection and associated diseases. Oncogene. 2005; 24(39):6058–6068. doi:10.1038/sj.onc.1208968.

4. Pique C, Jones K. Pathways of cell-cell transmission of HTLV-1. Frontiers in Microbiology [Internet]. 2012 [cited 2022 Apr 4]; 3. Available from: https://www.frontiersin.org/article/10.3389/fmicb.2012.00378.

5. Donegan E, Lee H, Operskalski E a., Shaw G m., Kleinman S h., Busch M p., et al. Transfusion transmission of retroviruses: human T-lymphotropic virus types I and II compared with human immunodeficiency virus type 1. Transfusion. 1994; 34(6):478–483. doi:10.1046/j.1537-2995.1994.34694295061.x.

6. Gessain A, Cassar O. Epidemiological Aspects and World Distribution of HTLV-1 Infection. Front Microbiol. 2012; 3:388. doi:10.3389/fmicb.2012.00388.

7. Murphy EL, Hanchard B, Figueroa JP, Gibbs WN, Lofters WS, Campbell M, et al. Modelling the risk of adult T-cell leukemia/lymphoma in persons infected with human T-lymphotropic virus type I. International Journal of Cancer. 1989; 43(2):250–253. doi:10.1002/ijc.2910430214.

8. Kaplan JE, Osame M, Kubota H, Igata A, Nishitani H, Maeda Y, et al. The risk of development of HTLV-I-associated myelopathy/tropical spastic paraparesis among persons infected with HTLV-I. J Acquir Immune Defic Syndr (1988). 1990; 3(11):1096–1101.

9. Schierhout G, McGregor S, Gessain A, Einsiedel L, Martinello M, Kaldor J. Association between HTLV-1 infection and adverse health outcomes: a systematic review and meta-analysis of epidemiological studies. The Lancet Infectious Diseases. 2020; 20(1):133–143. doi:10.1016/S1473-3099(19)30402-5.

10. Nagasaka M, Yamagishi M, Yagishita N, Araya N, Kobayashi S, Makiyama J, et al. Mortality and risk of progression to adult T cell leukemia/lymphoma in HTLV-1–associated myelopathy/tropical spastic paraparesis. PNAS. 2020; 117(21):11685–11691. doi:10.1073/pnas.1920346117.

11. Gonçalves DU, Proietti FA, Ribas JGR, Araújo MG, Pinheiro SR, Guedes AC, et al. Epidemiology, Treatment, and Prevention of Human T-Cell Leukemia Virus Type 1-Associated Diseases. Clin Microbiol Rev. 2010; 23(3):577–589. doi:10.1128/CMR.00063-09.

12. Martin F, Taylor GP, Jacobson S. Inflammatory manifestations of HTLV-1 and their therapeutic options. Expert Review of Clinical Immunology. 2014; 10(11):1531–1546. doi:10.1586/1744666X.2014.966690.

13. Iwanaga M, Watanabe T, Utsunomiya A, Okayama A, Uchimaru K, Koh K-R, et al. Human T-cell leukemia virus type I (HTLV-1) proviral load and disease progression in asymptomatic HTLV-1 carriers: a nationwide prospective study in Japan. Blood. 2010; 116(8):1211–1219. doi:10.1182/blood-2009-12-257410.

14. Watanabe T. Adult T-cell leukemia: molecular basis for clonal expansion and transformation of HTLV-1–infected T cells. Blood. 2017; 129(9):1071–1081. doi:10.1182/blood-2016-09-692574.

15. Kannian P, Green PL. Human T Lymphotropic Virus Type 1 (HTLV-1): Molecular Biology and Oncogenesis. Viruses. 2010; 2(9):2037–2077. doi:10.3390/v2092037.

16. Ohtani K, Iwanaga R, Arai M, Huang Y, Matsumura Y, Nakamura M. Cell Type-specific E2F Activation and Cell Cycle Progression Induced by the Oncogene Product Tax of Human T-cell Leukemia Virus Type I*. Journal of Biological Chemistry. 2000; 275(15):11154–11163. doi:10.1074/jbc.275.15.11154.

17. Currer R, Van Duyne R, Jaworski E, Guendel I, Sampey G, Das R, et al. HTLV Tax: A Fascinating Multifunctional Co-Regulator of Viral and Cellular Pathways. Frontiers in Microbiology [Internet]. 2012 [cited 2022 Apr 5]; 3. Available from: https://www.frontiersin.org/article/10.3389/fmicb.2012.00406.

18. Ahlers JD, Belyakov IM, Terabe M, Koka R, Donaldson DD, Thomas EK, et al. A push–pull approach to maximize vaccine efficacy: Abrogating suppression with an IL-13 inhibitor while augmenting help with granulocyte/macrophage colony-

stimulating factor and CD40L. Proceedings of the National Academy of Sciences. 2002; 99(20):13020–13025. doi:10.1073/pnas.192251199.

19. Kao S-Y, Lemoine FJ, Marriott SJ. HTLV-1 Tax protein sensitizes cells to apoptotic cell death induced by DNA damaging agents. Oncogene. 2000; 19(18):2240–2248. doi:10.1038/sj.onc.1203559.

20. Grossman WJ, Kimata JT, Wong FH, Zutter M, Ley TJ, Ratner L. Development of leukemia in mice transgenic for the tax gene of human T-cell leukemia virus type I. Proceedings of the National Academy of Sciences. 1995; 92(4):1057–1061. doi:10.1073/pnas.92.4.1057.

21. Masumoto K, Shibata H, Fujisawa J, Inoue H, Hakura A, Tsukahara T, et al. Human T-Cell Leukemia Virus Type 1 Tax Protein Transforms Rat Fibroblasts via Two Distinct Pathway. Journal of Virology. 1997; 71(6):4445–4451. doi:10.1128/jvi.71.6.4445-4451.1997.

22. Tanaka A, Takahashi C, Yamaoka S, Nosaka T, Maki M, Hatanaka M. Oncogenic transformation by the tax gene of human T-cell leukemia virus type I in vitro. Proceedings of the National Academy of Sciences. 1990; 87(3):1071–1075. doi:10.1073/pnas.87.3.1071.

23. Tang S-W, Chen C-Y, Klase Z, Zane L, Jeang K-T. The Cellular Autophagy Pathway Modulates Human T-Cell Leukemia Virus Type 1 Replication. J Virol. 2013; 87(3):1699–1707. doi:10.1128/JVI.02147-12.

24. Satou Y, Yasunaga J, Yoshida M, Matsuoka M. HTLV-I basic leucine zipper factor gene mRNA supports proliferation of adult T cell leukemia cells. Proceedings of the National Academy of Sciences. 2006; 103(3):720–725. doi:10.1073/pnas.0507631103.

25. Zhao T, Matsuoka M. HBZ and its roles in HTLV-1 oncogenesis. Front Microbiol. 2012; 3:247. doi:10.3389/fmicb.2012.00247.

26. Zhao T, Yasunaga J, Satou Y, Nakao M, Takahashi M, Fujii M, et al. Human T-cell leukemia virus type 1 bZIP factor selectively suppresses the classical pathway of NF-kappaB. Blood. 2009; 113(12):2755–2764. doi:10.1182/blood-2008-06-161729.

27. Mukai R, Ohshima T. HTLV-1 HBZ positively regulates the mTOR signaling pathway via inhibition of GADD34 activity in the cytoplasm. Oncogene. 2014; 33(18):2317–2328. doi:10.1038/onc.2013.181.

28. Schmeisser K, Parker JA. Pleiotropic Effects of mTOR and Autophagy During Development and Aging. Frontiers in Cell and Developmental Biology [Internet].

2019 [cited 2022 Apr 5]; 7. Available from: https://www.frontiersin.org/article/10.3389/fcell.2019.00192.

29. Satou Y, Yasunaga J, Zhao T, Yoshida M, Miyazato P, Takai K, et al. HTLV-1 bZIP Factor Induces T-Cell Lymphoma and Systemic Inflammation In Vivo. PLOS Pathogens. 2011; 7(2):e1001274. doi:10.1371/journal.ppat.1001274.

30. Saito M, Matsuzaki T, Satou Y, Yasunaga J, Saito K, Arimura K, et al. In vivo expression of the HBZ gene of HTLV-1 correlates with proviral load, inflammatory markers and disease severity in HTLV-1 associated myelopathy/tropical spastic paraparesis (HAM/TSP). Retrovirology. 2009; 6(1):19. doi:10.1186/1742-4690-6-19.

31. Matsuoka M, Jeang K-T. Human T-cell leukaemia virus type 1 (HTLV-1) infectivity and cellular transformation. Nat Rev Cancer. 2007; 7(4):270–280. doi:10.1038/nrc2111.

32. Miyazaki M, Yasunaga J-I, Taniguchi Y, Tamiya S, Nakahata T, Matsuoka M. Preferential Selection of Human T-Cell Leukemia Virus Type 1 Provirus Lacking the 5′ Long Terminal Repeat during Oncogenesis. Journal of Virology. 2007; 81(11):5714–5723. doi:10.1128/JVI.02511-06.

33. Takeda S, Maeda M, Morikawa S, Taniguchi Y, Yasunaga J, Nosaka K, et al. Genetic and epigenetic inactivation of tax gene in adult T-cell leukemia cells. International Journal of Cancer. 2004; 109(4):559–567. doi:10.1002/ijc.20007.

34. Mahgoub M, Yasunaga J, Iwami S, Nakaoka S, Koizumi Y, Shimura K, et al. Sporadic on/off switching of HTLV-1 Tax expression is crucial to maintain the whole population of virus-induced leukemic cells. PNAS. 2018; 115(6):E1269–E1278. doi:10.1073/pnas.1715724115.

35. Pegtel DM, Cosmopoulos K, Thorley-Lawson DA, van Eijndhoven MAJ, Hopmans ES, Lindenberg JL, et al. Functional delivery of viral miRNAs via exosomes. Proceedings of the National Academy of Sciences. 2010; 107(14):6328–6333. doi:10.1073/pnas.0914843107.

36. Campbell TD, Khan M, Huang M-B, Bond VC, Powell MD. HIV-1 Nef Protein Is Secreted into Vesicles That Can Fuse with Target Cells and Virions. Ethn Dis. 2008; 18(2 0 2):S2-14–9.

37. Narayanan A, Iordanskiy S, Das R, Duyne RV, Santos S, Jaworski E, et al. Exosomes Derived from HIV-1-infected Cells Contain Trans-activation Response Element RNA *. Journal of Biological Chemistry. 2013; 288(27):20014–20033. doi:10.1074/jbc.M112.438895.

38. Jaworski E, Narayanan A, Van Duyne R, Shabbeer-Meyering S, Iordanskiy S, Saifuddin M, et al. Human T-lymphotropic Virus Type 1-infected Cells Secrete Exosomes That Contain Tax Protein*. Journal of Biological Chemistry. 2014; 289(32):22284–22305. doi:10.1074/jbc.M114.549659.

39. Gill S, Catchpole R, Forterre P. Extracellular membrane vesicles in the three domains of life and beyond. FEMS Microbiology Reviews. 2019; 43(3):273–303. doi:10.1093/femsre/fuy042.

40. Johnstone RM. Maturation of reticulocytes: formation of exosomes as a mechanism for shedding membrane proteins. Biochem. Cell Biol. 1992; 70(3–4):179–190. doi:10.1139/o92-028.

41. Yáñez-Mó M, Siljander PR-M, Andreu Z, Zavec AB, Borràs FE, Buzas EI, et al. Biological properties of extracellular vesicles and their physiological functions. J Extracell Vesicles. 2015; 4:27066. doi:10.3402/jev.v4.27066.

42. Zaborowski MP, Balaj L, Breakefield XO, Lai CP. Extracellular Vesicles: Composition, Biological Relevance, and Methods of Study. BioScience. 2015; 65(8):783–797. doi:10.1093/biosci/biv084.

43. Cotzomi-Ortega I, Aguilar-Alonso P, Reyes-Leyva J, Maycotte P. Autophagy and Its Role in Protein Secretion: Implications for Cancer Therapy. Mediators of Inflammation. 2018; 2018:e4231591. doi:10.1155/2018/4231591.

44. Pleet ML, Branscome H, DeMarino C, Pinto DO, Zadeh MA, Rodriguez M, et al. Autophagy, EVs, and Infections: A Perfect Question for a Perfect Time. Front. Cell. Infect. Microbiol. [Internet]. 2018 [cited 2020 Oct 28]; 8. doi:10.3389/fcimb.2018.00362.

45. Tkach M, Kowal J, Zucchetti AE, Enserink L, Jouve M, Lankar D, et al. Qualitative differences in T-cell activation by dendritic cell-derived extracellular vesicle subtypes. EMBO J. 2017; 36(20):3012–3028. doi:10.15252/embj.201696003.

46. Crescitelli R, Lässer C, Szabó TG, Kittel A, Eldh M, Dianzani I, et al. Distinct RNA profiles in subpopulations of extracellular vesicles: apoptotic bodies, microvesicles and exosomes. Journal of Extracellular Vesicles. 2013; 2(1):20677. doi:10.3402/jev.v2i0.20677.

47. Kowal J, Arras G, Colombo M, Jouve M, Morath JP, Primdal-Bengtson B, et al. Proteomic comparison defines novel markers to characterize heterogeneous populations of extracellular vesicle subtypes. Proc Natl Acad Sci U S A. 2016; 113(8):E968–E977. doi:10.1073/pnas.1521230113.

48. Heijnen HF, Schiel AE, Fijnheer R, Geuze HJ, Sixma JJ. Activated platelets release two types of membrane vesicles: microvesicles by surface shedding and exosomes derived from exocytosis of multivesicular bodies and alpha-granules. Blood. 1999; 94(11):3791–3799.

49. Zhang Q, Higginbotham JN, Jeppesen DK, Yang Y-P, Li W, McKinley ET, et al. Transfer of Functional Cargo in Exomeres. Cell Reports. 2019; 27(3):940-954.e6. doi:10.1016/j.celrep.2019.01.009.

50. Théry C, Amigorena S, Raposo G, Clayton A. Isolation and Characterization of Exosomes from Cell Culture Supernatants and Biological Fluids. Current Protocols in Cell Biology. 2006; 30(1):3.22.1-3.22.29. doi:https://doi.org/10.1002/0471143030.cb0322s30.

51. Anderson MR, Pleet ML, Enose-Akahata Y, Erickson J, Monaco MC, Akpamagbo Y, et al. Viral antigens detectable in CSF exosomes from patients with retrovirus associated neurologic disease: functional role of exosomes. Clin Transl Med. 2018; 7:24. doi:10.1186/s40169-018-0204-7.

52. Pinto DO, DeMarino C, Pleet ML, Cowen M, Branscome H, Al Sharif S, et al. HTLV-1 Extracellular Vesicles Promote Cell-to-Cell Contact. Front Microbiol. 2019; 10:2147. doi:10.3389/fmicb.2019.02147.

53. Pinto DO, Al Sharif S, Mensah G, Cowen M, Khatkar P, Erickson J, et al. Extracellular vesicles from HTLV-1 infected cells modulate target cells and viral spread. Retrovirology. 2021; 18(1):6. doi:10.1186/s12977-021-00550-8.

54. El-Saghir J, Nassar F, Tawil N, El-Sabban M. ATL-derived exosomes modulate mesenchymal stem cells: potential role in leukemia progression. Retrovirology. 2016; 13(1):73. doi:10.1186/s12977-016-0307-4.

55. Rahman MA, Barger JF, Lovat F, Gao M, Otterson GA, Nana-Sinkam P. Lung cancer exosomes as drivers of epithelial mesenchymal transition. Oncotarget. 2016; 7(34):54852–54866. doi:10.18632/oncotarget.10243.

56. Stefanius K, Servage K, de Souza Santos M, Gray HF, Toombs JE, Chimalapati S, et al. Human pancreatic cancer cell exosomes, but not human normal cell exosomes, act as an initiator in cell transformation. eLife. 2019; 8:e40226. doi:10.7554/eLife.40226.

57. Zeng A, Wei Z, Rabinovsky R, Jun HJ, Fatimy RE, Deforzh E, et al. Glioblastoma-Derived Extracellular Vesicles Facilitate Transformation of Astrocytes via Reprogramming Oncogenic Metabolism. iScience [Internet]. 2020 [cited 2021 Apr 9]; 23(8). doi:10.1016/j.isci.2020.101420.

58. Borowicz S, Van Scoyk M, Avasarala S, Karuppusamy Rathinam MK, Tauler J, Bikkavilli RK, et al. The Soft Agar Colony Formation Assay. J Vis Exp [Internet]. 2014 [cited 2021 Apr 9]; (92). doi:10.3791/51998.

59. Silverman JM, Reiner NE. Exosomes and other microvesicles in infection biology: organelles with unanticipated phenotypes. Cellular Microbiology. 2011; 13(1):1–9. doi:10.1111/j.1462-5822.2010.01537.x.

60. Ducasa N, Grasso D, Benencio P, Papademetrio DL, Biglione M, Kashanchi F, et al. Autophagy in Human T-Cell Leukemia Virus Type 1 (HTLV-1) Induced Leukemia. Frontiers in Oncology [Internet]. 2021 [cited 2022 Feb 25]; 11. Available from: https://www.frontiersin.org/article/10.3389/fonc.2021.641269.

61. Cao S, Maldonado JO, Grigsby IF, Mansky LM, Zhang W. Analysis of human T-cell leukemia virus type 1 particles by using cryo-electron tomography. J Virol. 2015; 89(4):2430–2435. doi:10.1128/JVI.02358-14.

62. Meissner ME, Mendonça LM, Zhang W, Mansky LM. Polymorphic Nature of Human T-Cell Leukemia Virus Type 1 Particle Cores as Revealed through Characterization of a Chronically Infected Cell Line. J Virol. 2017; 91(16):e00369-17. doi:10.1128/JVI.00369-17.

63. Yamagishi M, Watanabe T. Molecular Hallmarks of Adult T Cell Leukemia. Front Microbiol. 2012; 3:334. doi:10.3389/fmicb.2012.00334.

64. Huang J, Ding Z, Luo Q, Xu W. Cancer cell-derived exosomes promote cell proliferation and inhibit cell apoptosis of both normal lung fibroblasts and non-small cell lung cancer cell through delivering alpha-smooth muscle actin. Am J Transl Res. 2019; 11(3):1711–1723.

65. Bereiter-Hahn J, Münnich A, Woiteneck P. Dependence of Energy Metabolism on the Density of Cells in Culture. Cell Structure and Function. 1998; 23(2):85–93. doi:10.1247/csf.23.85.

66. Deng Z, Wang H, Liu J, Deng Y, Zhang N. Comprehensive understanding of anchorage-independent survival and its implication in cancer metastasis. Cell Death Dis. 2021; 12(7):1–12. doi:10.1038/s41419-021-03890-7.

67. Jolly MK, Ware KE, Xu S, Gilja S, Shetler S, Yang Y, et al. E-cadherin represses anchorage-independent growth in sarcomas through both signaling and mechanical mechanisms. Mol Cancer Res. 2019; 17(6):1391–1402. doi:10.1158/1541-7786.MCR-18-0763.

68. Kagdi H, Demontis MA, Ramos JC, Taylor GP. Switching and loss of cellular cytokine producing capacity characterize in vivo viral infection and malignant

transformation in human T- lymphotropic virus type 1 infection. PLoS Pathog. 2018; 14(2):e1006861. doi:10.1371/journal.ppat.1006861.

69. Otaguiri KK, dos Santos DF, Slavov SN, Depieri LV, Palma PVB, Meirelles FV, et al. *TAX* -mRNA-Carrying Exosomes from Human T Cell Lymphotropic Virus Type 1-Infected Cells Can Induce Interferon-Gamma Production *In Vitro*. AIDS Research and Human Retroviruses. 2018; 34(12):1075–1082. doi:10.1089/aid.2018.0115.

BIOGRAPHY

Zachary Cuba graduated from the Commonwealth Governor's School Program at Spotsylvania High School, Spotsylvania, Virginia, in 2016. He received his Bachelor of Science in Biology from the College of William and Mary in 2020, after spending three years researching auxiliary metabolic genes in aquatic and soil bacteriophage in the Viral Ecology Lab under Dr. Kurt Williamson. He then was accepted into GMU's School of Systems Biology, allowing him to pursue a Master of Biology with a concentration in Microbiology and Infectious Disease in 2022.

Under the mentorship of Dr. Fatah Kashanchi and the members of the Laboratory of Molecular Virology, Zach gained several skills and experiences: in addition to his work with EVs, he was trained to work in BSL3 conditions with SARS-CoV-2, he presented a poster on coronavirus EVs at the American Society of Intercellular Communication Fall 2020 conference, and he contributed to a paper from Dr. Lance Liotta's lab on breast cancer interstitial fluid EVs.

After graduation, Zach has accepted a position as a Biologist at the International Reagent Resource at the American Type Culture Collection in Manassas, VA.